Florian Lipsmeier · Ellen Baake

Rare event simulation for T-cell activation

Abstract The problem of *statistical recognition* is considered, as it arises in immunobiology, namely, the discrimination of foreign antigens against a background of the body's own molecules. The precise mechanism of this foreign-self-distinction, though one of the major tasks of the immune system, continues to be a fundamental puzzle. Recent progress has been made by van den Berg, Rand, and Burroughs [33], who modelled the *probabilistic* nature of the interaction between the relevant cell types, namely, T-cells and antigen-presenting cells (APCs). Here, the stochasticity is due to the random sample of antigens present on the surface of every APC, and to the random receptor type that characterises individual T-cells. It has been shown previously [33,37] that this model, though highly idealised, is capable of reproducing important aspects of the recognition phenomenon, and of explaining them on the basis of stochastic rare events. These results were obtained with the help of a refined large deviation theorem and were thus asymptotic in nature. Simulations have, so far, been restricted to the straightforward simple sampling approach, which does not allow for sample sizes large enough to address more detailed questions. Building on the available large deviation results, we develop an importance sampling technique that allows for a convenient exploration of the relevant tail events by means of simulation. With its help, we investigate the mechanism of statistical recognition in some depth. In particular, we illustrate how a foreign antigen can stand out against the self background if it is present in sufficiently many copies, although no *a priori* difference between self and nonself is built into the model.

Keywords Immunobiology · statistical recognition · large deviations · rare event simulation

PACS 87.16.af · 87.16.dr · 87.18.Tt

Mathematics Subject Classification (2000) 92-08 · 92C99 · 60F10

1 Introduction

The notion of statistical recognition between randomly encountered molecules is central to many biological phenomena. This is particularly evident in biological repertoires, which contain enough molecular diversity to bind practically any randomly encountered target molecule. The receptor repertoire of the immune system provides the best-known example of a system displaying probability-based interactions; another one is the olfactory receptor repertoire, which recognises multitudes of odorants. This chance recognition is a well-established phenomenon and has been

F. Lipsmeier, E. Baake
Faculty of Technology, Bielefeld University, 33501 Bielefeld, Germany
E-mail: {flipsmei,ebaake}@techfak.uni-bielefeld.de

analysed with the help of various statistical and biophysical models; compare [17,23]. Here we will tackle a model of statistical recognition between *cell surfaces* (in the sense of collections of numerous surface molecules, rather than single ones) of the immune system. It describes a vital property of our immune system, which comes into play when a virus invades the body and starts to multiply. Fortunately, however, sooner or later it is recognised as a foreign intruder by certain white blood cells, which are part of the immune system and start a specific immune response that finally eliminates the virus population.

This ability of the immune system to discriminate safely between foreign and self molecules is a fundamental ingredient to everyday survival of jawed vertebrates; but how this works exactly is still enigmatic. Indeed, the immune system faces an enormous challenge because it must recognise one (or a few) type(s) of (potentially dangerous) foreign molecules against an enormous variety of (harmless) self molecules. The particular difficulty lies in the fact that there can be no a priori difference between self and nonself (like some fundamental difference in molecular structure), since this would open up the possibility for molecular mimicry on the part of the pathogen, which could quickly evolve immuno-invisibility by imitating the self structure. The problem may be phrased as *statistical recognition* of one particular foreign signal against a large, fluctuating self background. However, immune biology has been largely treated deterministically until, recently, an explicit stochastic model was introduced by van den Berg, Rand and Burroughs [33] (henceforth referred to as BRB) and further developed by Zint, Baake and den Hollander [37]. It describes (random) encounters between the two crucial types of white blood cells involved (see Figs. 1 and 2): the antigen-presenting cells (APCs), which display a mixture of self and foreign antigens at their surface (a sample of the molecules around in the body), and the T-cells, which "scan" the APCs by means of certain receptors and ultimately decide whether or not to react, i.e., to start an immune response.
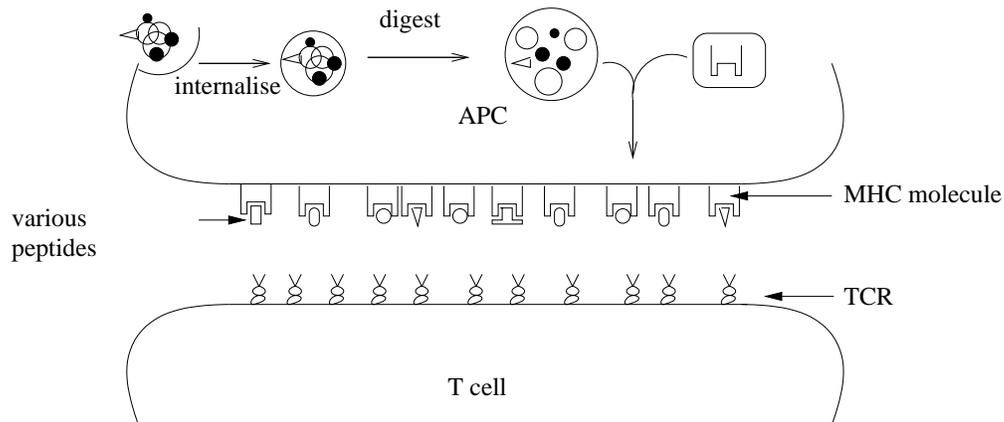

Fig. 1 A T-cell and an antigen-presenting cell (based on Fig. 1 of [35]). An *APC* absorbs molecules and particles from its vicinity and breaks them down. The emerging fragments, so-called peptides (short sequences of amino acids), serve as antigens. They are bound to so-called MHC molecules (still within the cell), and the resulting complexes, each composed of an MHC molecule and a peptide, are presented on the surface of the cell (the MHC molecules serve as carriers or anchors to the cell surface). Since most of the molecules in the vicinity of an APC are self molecules, every APC displays a large variety of different types of self antigens and, possibly, one (or a small number of) foreign types. The various antigen types occur in various copy numbers. Each *T-cell* is characterised by a specific type of T-cell receptor (TCR), which is displayed in many *identical* copies on the surface of the particular T-cell. When a T-cell meets an APC, the contact between them is established by a temporary bond between the cells, in which the TCRs and the MHC-peptide complexes interact with each other, which results in stimuli to the T-cell body. If the added stimulation rate is above a given threshold, the T-cell is activated to reproduce, and the resulting clones of T-cells will initiate an immune reaction against the intruder.

To be biologically more precise, we consider the encounters of so-called *naive T-cells* with *professional APCs* in the *secondary lymphoid tissue*. A *naive T-cell* is a cell that has finished its maturation process in the thymus and has been released into the body, where it has not yet been exposed to antigen. It tends to dwell in *secondary lymphoid tissue* like lymph nodes, where it comes into contact with *professional APCs*, special white blood cells with so-called MHC molecules at their surface that serve as carriers for antigens. Each *T-cell* is characterised by a specific type of T-cell receptor (TCR), which is displayed in many *identical* copies on the surface of the particular T-cell. A large number (estimated at 10^7 in [1]) of different receptors, and hence different T-cell types, are present in an individual (every type, in turn, is present in several copies, which form a T-cell clone). However, the number of potential antigen types is still vastly larger (roughly 10^{13}; see [20]). Thus, specific recognition (where one TCR recognises exactly one antigen) is impossible; this is known as Mason's paradox. The task is further complicated by the fact that every APC displays on the order of thousand(s) of different self antigen types, in various copy numbers [14, 20,28], together with, possibly, one (or a small number of) foreign types; the T-cells therefore face a literal "needle in a haystack" problem.

For an encounter between a pair of T-cell and APC, both chosen randomly from the diverse pool of T-cells and APCs, the probability to react must be very small (otherwise, immune reactions would occur permanently); this is a central theme in the analysis. It entails that some questions may be answered analytically with the help of large deviation theory; others require simulation, but the use of this has been limited due to the small probabilities involved, at least with the straightforward simulation methods applied so far [33,37]. The main purpose of this article is to devise an efficient importance sampling method based on large deviation theory and tailored to the problem at hand, and to use this to investigate the mechanism of statistical recognition in more detail. The paper is organised as follows. In Sect. 2, we present the most important biological facts and recapitulate the model; this will be a self-contained, but highly simplified outline, since the full picture is available elsewhere [33,37]. In Sect. 3, we summarise (mainly from [9] and [5]) some general theory that allows to design efficient methods of rare event simulation on the basis of a large deviation analysis, and tailor these to the problem at hand in Sect. 4. Sect. 5 presents the simulation results and analyses them both from the computational and the biological point of view. Simulation speeds up by a factor of nearly 1500 relative to the straightforward approaches used so far. This enables us to explore regions of parameter space as yet inaccessible, to validate previous asymptotic results, and to investigate the mechanism of statistical recognition in more depth than previously possible.

2 The T-cell model

In this Section, we briefly motivate and introduce the model of T-cell recognition as first proposed by BRB in 2001 [33] and further developed by Zint, Baake and den Hollander [37]. More precisely, we only consider the toy version of this model, which neglects the modification of the T-cell repertoire during maturation in the thymus. This toy version already captures important aspects of the phenomenon while being particularly transparent. We will come back to maturation (already included in [33]) in the discussion.

When T-cells and APCs meet, the T-cell receptors bind to the various antigens presented by the APC [6]. For every single receptor-antigen pair, there is an association-dissociation reaction, the rate constants for which depend on the match of the molecular structures of receptor and antigen. Assuming that association is much faster than dissociation and that there is an abundance of receptors (so that the antigens are mostly in the bound state), one can describe the reaction in terms of the dissociation rates only.

Every time a receptor unbinds from an antigen, it sends a signal to the T-cell, provided the association has lasted for at least one time unit (i.e., we rescale time so that the unit of time is this minimal association time required). The duration of a binding of a given receptor-antigen pair follows the $\text{Exp}(1/\tau)$ distribution, i.e. the exponential distribution with mean τ, where τ is the inverse dissociation rate of the pair in question. The rate of stimuli induced by the interaction of
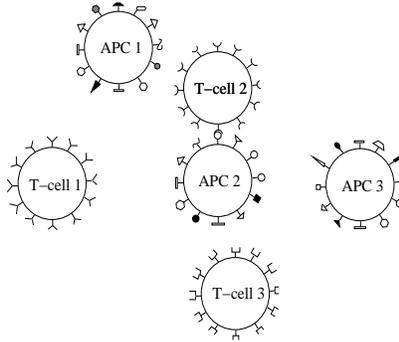
Fig. 2 Caricature of T-cells and APCs (from [37]). Note that every T-cell has many copies of one particular receptor type, but different T-cells have different receptor types. In contrast, every APC carries a mixture of antigen types, which may appear in various copy numbers.

our antigen with the receptors in its vicinity is then given by

$$w(\tau) = \frac{1}{\tau} \exp(-\frac{1}{\tau}), \tag{1}$$

i.e., the dissociation rate times the probability that the association has lasted long enough. (If the simplifying assumption of unlimited receptor abundance is dispensed with, Eq. (1) must be modified, see [34].) As shown in Fig. 3, the function w first increases and then decreases with τ with a maximum at $\tau = 1$, which reflects the fact that, for $\tau < 1$, the bindings tend not to last long enough, whereas for $\tau > 1$, they tend to last so long that only few stimuli are expected per time unit.
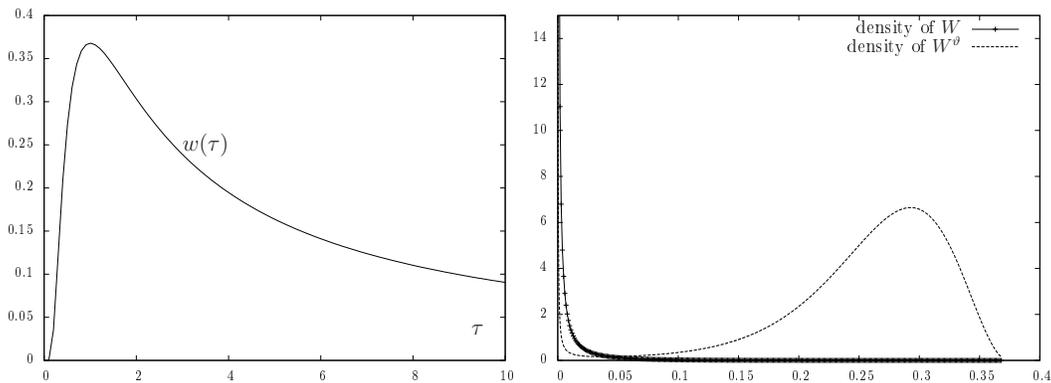

Fig. 3 Left: the function w. Right: the densities of $W = w(\mathcal{T})$ and W^ϑ with tilting parameter $\vartheta = 46$ (cf. Sect. 3.2). The densities have poles at $w(0) = 0$ and $w(1) = 0.3679$ (due to the vanishing derivative of w at $\tau = 0$ and $\tau = 1$), but the right poles are invisible because they support very little probability mass. In fact, for $\varepsilon = 0.01$, one has $\mathbb{P}(0 \leq W \leq \varepsilon) = 0.98$ and $\mathbb{P}(w(1) - \varepsilon \leq W \leq w(1)) = 2.17 \cdot 10^{-9}$, whereas $\mathbb{P}(0 \leq W^\vartheta \leq \varepsilon) = 0.137138$ and $\mathbb{P}(w(1) - \varepsilon \leq W^\vartheta \leq w(1)) = 0.0050$.

The T-cell sums up the signals induced by the different antigens on the APC, and if the total stimulation rate reaches a certain threshold value, the cell initiates an immune response. This model relies on several hypotheses, which are known as kinetic proofreading [21,22,18,13], serial triggering [31,30,27,4,29,10], counting of stimulated TCRs [36,25], and the optimal dwell-time hypothesis [15,12].

Due to the huge amount of different receptor and antigen types, it is impossible (and unnecessary) to prescribe the binding durations for all pairs of receptor and antigen types individually. Therefore, BRB chose a probabilistic approach to describe the meeting of APCs and T-cells. A randomly chosen T-cell (that is, a randomly chosen type of receptor) encounters a randomly chosen APC (that is, a random mixture of antigens). The mean binding time that governs the binding of this random receptor to the jth type of antigen is taken to be a random variable denoted by $\mathcal{T}_j$. The $\mathcal{T}_j$ are independent and identically distributed (i.i.d.) and are assumed to follow the $\mathrm{Exp}(1/\bar{\tau})$ distribution, i.e., the exponential distribution with mean $\bar{\tau}$, where $\bar{\tau}$ is a free parameter. Note that there are two exponential distributions (and two levels of averaging) involved here. First, the duration of an *individual binding* between a type-j antigen and a random receptor is $\mathrm{Exp}(1/\mathcal{T}_j)$ distributed (see the discussion of Eq. (1)). Second, $\mathcal{T}_j$, the *mean duration* of such a binding (where the receptor is chosen once and the times are averaged over repeated bindings with a j antigen) is itself an exponential random variable, with realisation τ_j. Finally, its mean, $\mathbb{E}(\mathcal{T}_j) = \bar{\tau}$, is the mean binding time of a j-antigen (and, due to the i.i.d. assumption, of any antigen) when averaged over all encounters with the various receptor types. The exponential distribution of the individual binding time is an immediate consequence of the (first-order) unbinding kinetics. In contrast, the corresponding assumption for the $\mathcal{T}_j$ is made for simplicity; the approach is compatible with various other distributions as well, see [33] and [37]. The i.i.d. assumption, however, is crucial, since it implies, in particular, that there is no difference between self and foreign antigens here; i.e., no a priori distinction is built into the model.

The total stimulation a T-cell receives is the sum over all stimulus rates $W_j = w(\mathcal{T}_j)$ that emerge from antigens of the j'th type. It is further assumed that there is at most one type of foreign antigen in $z^{(f)}$ copies on an APC, whose signal must be discriminated against the signals of a huge amount of self antigens. (There could, in principle, be multiple foreign peptide types, but there are good reasons to assume that there are mechanisms to ensure that a given T-cell sees at most one foreign peptide type, see [34]). The self antigens are here divided into two distinct classes, c and v, that are present in different copy numbers $z^{(c)}$ and $z^{(v)}$. An APC displays $m^{(c)}$ and $m^{(v)}$ different types of class c and v. The indices c and v stand for constitutive and for variable, respectively; but for the purpose of this article, only the abundancies are relevant, in particular, $z^{(c)} > z^{(v)}$ and $m^{(c)} < m^{(v)}$. Over the whole APC the total number of antigens is then $m^{(c)}z^{(c)} + m^{(v)}z^{(v)} =: M$ if no foreign antigen is present. If $z^{(f)}$ foreign molecules are also present, the self molecules are assumed to be proportionally displaced (via the factor $q := (M - z^{(f)})/M$), so that the total number of antigens remains unchanged at

$$z^{(f)} + m^{(c)}qz^{(c)} + m^{(v)}qz^{(v)} = M. \tag{2}$$

The total stimulation rate in a random encounter of T-cell and APC can then be described as a function of $z^{(f)}$:

$$G(z^{(f)}) := \left(\sum_{j=1}^{m^{(c)}} qz^{(c)}W_j\right) + \left(\sum_{j=m^{(c)}+1}^{m^{(c)}+m^{(v)}} qz^{(v)}W_j\right) + z^{(f)}W_{m^{(c)}+m^{(v)}+1}, \tag{3}$$

i.e., a weighted sum of i.i.d. random variables. Alternatively, we consider the extension of the model proposed by Zint et al. [37], which, instead of the deterministic copy numbers $z^{(c)}, z^{(v)}$, uses random variables $Z_j^{(c)}, Z_j^{(v)}$ distributed according to binomial distributions with $\mathbb{E}(Z_j^{(c)}) = z^{(c)}$, $\mathbb{E}(Z_j^{(v)}) = z^{(v)}$, where $\mathbb{E}$ denotes expectation (so the expected number of antigens per APC is still M). The model then reads

$$G(z^{(f)}) := \left(\sum_{j=1}^{m^{(c)}} qZ_j^{(c)}W_j\right) + \left(\sum_{j=m^{(c)}+1}^{m^{(c)}+m^{(v)}} qZ_j^{(v)}W_j\right) + z^{(f)}W_{m^{(c)}+m^{(v)}+1}. \tag{4}$$

In line with [33,37], we numerically specify the model parameters as follows: $\bar{\tau} = 0.04$; $m^{(c)} = 50$, $m^{(v)} = 1500$, $z^{(c)} = 500$, $z^{(v)} = 50$ (and hence $M = 10^5$). The distributions in the extended

model are the binomials $\mathrm{Bin}(\zeta^{(c)}, p)$ and $\mathrm{Bin}(\zeta^{(v)}, p)$ for $Z_j^{(c)}$ and $Z_j^{(v)}$ respectively, where $\zeta^{(c)} = 1000$, $\zeta^{(v)} = 100$, and $p = 0.5$.

The relevant quantity for us is now the probability

$$\mathbb{P}\big(G(z^{(f)}) \geq g_{\mathrm{act}}\big) \tag{5}$$

that the stimulation rate reaches or surpasses a threshold g_{act}. To achieve a good foreign-self discrimination, there must be a large difference in probability between the stimulation rate in the case with self antigens only $(z^{(f)} = 0)$, and the stimulation rate with the foreign antigen present, i.e.,

$$1 \gg \mathbb{P}\big(G(z^{(f)}) \geq g_{\mathrm{act}}\big) \gg \mathbb{P}\big(G(0) \geq g_{\mathrm{act}}\big) \geq 0 \tag{6}$$

for realistic values of $z^{(f)}$. Note that both events must be rare events – otherwise, the immune system would "fire" all the time. Thus g_{act} must be much larger than $\mathbb{E}(G(z^{(f)}))$ (which, due to (2) and the identical distribution of the W_j, is independent of $z^{(f)}$). Evaluating these small probabilities is a challenge. So far, two routes have been used: analytic (asymptotic) theory based on large deviations (LD) and straightforward simulation (so-called simple sampling). Both have their shortcomings: the LD approach is only exact in the limit of infinitely many antigen types (and the available error estimates are usually too crude to be useful); the simulation strategy, on the other hand, is so time-consuming that it becomes simply impossible to obtain sample sizes large enough for a detailed analysis, in particular for large values of g_{act}. Therefore, an importance sampling approach is required. Let us now recapitulate some underlying theory.

3 Rare event simulation: general theory

The general problem we now consider is to estimate the probability $P(A)$ of a (rare) event A under a probability measure P. The straightforward approach, known as simple sampling, uses the estimate

$$(\widehat{P(A)})_N := \frac{1}{N}\sum_{i=1}^{N} \mathbb{1}\{S^{(i)} \in A\} = \frac{1}{N}\mathrm{card}\{1 \leq i \leq N \mid S^{(i)} \in A\}, \tag{7}$$

where the $\{S^{(i)}\}_{1 \leq i \leq N}$ are independent and identically distributed (i.i.d.) random variables with distribution P, $\mathbb{1}\{.\}$ denotes the indicator function, and N is the sample size; we will throughout use $\widehat{v}$ for an estimate of a quantity v. $(\widehat{P(A)})_N$ is obviously an unbiased and consistent estimate, but, for small $P(A)$, the convergence to $P(A)$ is slow, and large samples are required to get reliable estimates.

Various simulation methods are available that deal with this problem and yield a better rate of convergence (see the monograph by Bucklew [5] for an overview). Most of them achieve this improvement by reducing the variance of the estimator. We will concentrate here on the most wide-spread class of methods, namely importance sampling. As is well known, one introduces a new sampling distribution Q here under which A is more likely to happen, produces samples from this distribution and returns to the original distribution by reweighting. In general, finding a good importance sampling distribution that reduces the variance as much as possible is an art, and much of the literature revolves around this. Some general purpose and many ad hoc strategies exist, but usually, importance sampling distributions are best tailored by exploiting the structure of the specific problem at hand. However, if the problem can be embedded into a sequence of problems for which a so-called large deviation principle is valid, a unified theory is available that identifies the most efficient simulation distribution. This technique of "large deviation simulation" was introduced by Sadowski and Bucklew [26], laid down in the monograph by Bucklew [5], and further developed by Dieker and Mandjes [9]. It rests on the well-established theory of large deviations, as summarised, for example, in the books by Dembo and Zeitouni [7] or den Hollander [8]. Let us recapitulate the basic background.

3.1 Large deviation probabilities

Consider a sequence $\{S_n\}$ of random variables on the probability space $(\mathbb{R}^d, \mathcal{B}, \mathbb{P})$, where $\mathcal{B}$ is the Borel σ-algebra of $\mathbb{R}^d$. Let $\{P_n\}$ be the family of probability measures induced by $\{S_n\}$, i.e., $P_n(B) = \mathbb{P}(S_n \in B)$ for $B \in \mathcal{B}$. We assume throughout that $\{S_n\}$ satisfies a large deviation principle (LDP) according to the following definition [7,9]:

Definition 1 (Large deviation principle) A family of probability measures $\{P_n\}$ on $(\mathbb{R}^d, \mathcal{B})$ satisfies the large deviation principle (LDP) with rate function I if $I : \mathbb{R}^d \to [0, \infty]$ is lower semicontinuous and, for all $B \in \mathcal{B}$,

$$- \inf_{x \in B^\circ} I(x) \le \liminf_{n \to \infty} \frac{1}{n} \log P_n(B) \le \limsup_{n \to \infty} \frac{1}{n} \log P_n(B) \le - \inf_{x \in \overline{B}} I(x), \tag{8}$$

where $B^\circ := \mathrm{int}(B)$ and $\overline{B} := \mathrm{clos}(B)$ denote the interior and the closure of B, respectively. I is said to be a good rate function if it has compact level sets in that $I^{-1}([0, c]) = \{x \in \mathbb{R}^d : I(x) \le c\}$ is compact for all $c \in \mathbb{R}^d$. $\square$

A set B is called an *I-continuity set* if

$$\inf_{x \in B^\circ} I(x) = \inf_{x \in B} I(x) = \inf_{x \in \overline{B}} I(x). \tag{9}$$

If B is such a set, the LDP means that $P_n(B)$ decays exponentially for large n, with decay coefficient $\inf_{x \in B} I(x)$. A point b is called a *minimum rate point* of B if $\inf_{x \in B} I(x) = I(b)$.

Large deviation principles are well known for many families of random variables, like empirical means of i.i.d. random variables or empirical measures of Markov chains. For the application we have in mind, which involves sums of independent, but not identically distributed random variables, we need the fairly general setting of the Gärtner-Ellis theorem, which we recapitulate here (cf. [7, Thm. 2.3.6] and [8, Ch. V]). Let $\varphi_n(\vartheta) := \mathbb{E}_{P_n}(e^{\langle \vartheta, S_n \rangle})$, $\vartheta \in \mathbb{R}^d$, be the moment-generating function of S_n, where $\langle ., . \rangle$ denotes the scalar product and $\mathbb{E}_\mu(.)$ denotes the expectation of a random variable with respect to the probability measure μ.

Theorem 1 (Gärtner-Ellis) *Assume that*

(G1) $\lim_{n \to \infty} \frac{1}{n} \log \varphi_n(n\vartheta) =: \Lambda(\vartheta) \in [-\infty, \infty]$ *exists,*
(G2) $0 \in \mathrm{int}(\mathcal{D}_\Lambda)$, *where $\mathcal{D}_\Lambda := \{\vartheta \in \mathbb{R}^d : \Lambda(\vartheta) < \infty\}$ is the* effective domain *of Λ,*
(G3) Λ *is lower semi-continuous on $\mathbb{R}^d$,*
(G4) Λ *is differentiable on* $\mathrm{int}(\mathcal{D}_\Lambda)$,
(G5) *Either $\mathcal{D}_\Lambda = \mathbb{R}^d$ or Λ is steep at its boundary $\partial \mathcal{D}_\Lambda$, i.e., $\lim_{\mathrm{int}(\mathcal{D}_\Lambda) \ni \vartheta \to \partial \mathcal{D}_\Lambda} |\nabla \Lambda(\vartheta)| = \infty$.*

Then, $\{P_n\}$ satisfies the LDP on $\mathbb{R}^d$ with good rate function I, where I is the Legendre transform of Λ, i.e.,

$$I(x) = \sup_{\vartheta \in \mathbb{R}^d} [\langle x, \vartheta \rangle - \Lambda(\vartheta)], \quad x \in \mathbb{R}^d. \tag{10}$$

$\square$

The function Λ in (G1) is convex. If there is a solution ϑ^* of

$$\nabla \Lambda(\vartheta) = x, \tag{11}$$

one has

$$I(x) = \langle \vartheta^*, x \rangle - \Lambda(\vartheta^*). \tag{12}$$

If Λ is strictly convex in all directions, ϑ^* is unique. See Fig. 4 for a one-dimensional example (the T-cell application, in fact).

3.2 Simulating rare event probabilities

Let now $A \in \mathcal{B}$ be a *rare event* in the sense that $0 < \inf_{x \in A} I(x) < \infty$. Here, the first inequality implies that A becomes exponentially unlikely as $n \to \infty$, whereas the second inequality serves to exclude nongeneric cases (in particular cases where the event is impossible). An important notion for the rare event simulation of $P_n(A)$ is that of a *dominating point* [5, p. 83]: A point a is a *dominating point* of the set A if it is the unique point such that

  a) $a \in \partial A$,
  b) $\exists$ a unique solution ϑ^* of $\nabla \Lambda(\vartheta) = a$, and
  c) $A \subset \{x \in \mathbb{R}^d : \langle \vartheta^*, x - a \rangle \geq 0\}$.

A dominating point, if it exists, is always a unique minimum rate point (see [5, p. 83]). Convexity of A implies existence of a dominating point (cf. [9]).

Following [9] we now turn to the problem of simulating $P_n(A) = \mathbb{E}_{P_n}(\mathbb{1}\{S_n \in A\})$. The naive simple-sampling estimate obtained from N i.i.d. copies $S_n^{(i)}$ ($1 \leq i \leq N$), drawn from P_n, is, as in (7), given by

$$\left(\widehat{P_n(A)} \right)_N := \frac{1}{N} \sum_{i=1}^{N} \mathbb{1}\{S_n^{(i)} \in A\}. \tag{13}$$

It is unbiased and converges (almost surely) to $P_n(A)$ in the limit $N \to \infty$, but it is inefficient since it requires that N increase exponentially with n to yield a meaningful estimate. Instead of $\{S_n\}$, one therefore considers an alternative family of random variables, $\{T_n\}$ with distribution family $\{Q_n\}$, again on $(\mathbb{R}^d, \mathcal{B})$, under which A occurs more frequently. Assuming that P_n and Q_n are absolutely continuous with respect to each other, one can use the identity

$$P_n(A) = \mathbb{E}_{P_n}(\mathbb{1}\{S_n \in A\}) = \mathbb{E}_{Q_n}\left(\mathbb{1}\{T_n \in A\} \frac{\mathrm{d}P_n}{\mathrm{d}Q_n}(T_n) \right), \tag{14}$$

where $\mathrm{d}P_n/\mathrm{d}Q_n$ is the Radon-Nikodym derivative of P_n with respect to Q_n. The resulting importance sampling estimate then relies on i.i.d. samples $T_n^{(i)}$ from $\{Q_n\}$ and reads

$$\left(\widehat{P_{Q_n}(A)} \right)_N := \frac{1}{N} \sum_{i=1}^{N} \mathbb{1}\{T_n^{(i)} \in A\} \frac{\mathrm{d}P_n}{\mathrm{d}Q_n}(T_n^{(i)}), \tag{15}$$

where $(\mathrm{d}P_n/\mathrm{d}Q_n)(.)$ acts as a reweighting factor from the sampling distribution to the original one. It is reasonable to assume that $(\mathrm{d}P_n/\mathrm{d}Q_n)$ is continuous to avoid the usual problems with L^1-functions; this is no restriction for our intended application.

An adequate optimality concept in this context is that of *asymptotic efficiency*. According to [9], it is based on the *relative error* $\eta_N(Q_n, A)$ defined via its square

$$\eta_N^2(Q_n, A) := \frac{\mathbb{V}_{Q_n}\left(\widehat{P_{Q_n}(A)} \right)_N}{\left(P_n(A) \right)^2} \tag{16}$$

(where $\mathbb{V}_\mu(.)$ denotes the variance of a random variable with respect to the probability measure μ). The relative error is proportional to the width of the confidence interval relative to the (expected) estimate itself. Asymptotic efficiency is then defined as follows.

Definition 2 (Asymptotic efficiency) An importance sampling family $\{Q_n\}$ is called *asymptotically efficient* for the rare event A if

$$\lim_{n \to \infty} \frac{1}{n} \log N_{Q_n}^* = 0, \tag{17}$$

where $N_{Q_n}^* := \inf\{N \in \mathbb{N} : \eta_N(Q_n, A) \leq \eta_{\max}\}$ for some given maximal relative error $\eta_{\max}$, $0 < \eta_{\max} < \infty$.

In words, asymptotic efficiency means that the number of samples required to keep the relative error below a prescribed bound $\eta_{\max}$ increases only subexponentially (rather than exponentially as with simple sampling). The concrete choice of $\eta_{\max}$ is actually irrelevant, see Lemma 1 in [9].

An obvious idea from large deviation theory would be to use, as sampling distributions, the family of measures $\{P_n^\vartheta\}$ that are exponentially tilted with parameter ϑ, that is,

$$\frac{\mathrm{d}P_n^\vartheta}{\mathrm{d}P_n}(x) = \frac{e^{n\langle \vartheta, x\rangle}}{\varphi_n(n\vartheta)}, \quad x \in \mathbb{R}^d; \tag{18}$$

P_n^ϑ then takes the role of Q_n. The task remains to find a suitable ϑ, i.e., a tilting parameter that makes $\{P_n^\vartheta\}$ asymptotically efficient. Necessary and sufficient conditions for this are given in [9, Assumption 1 and Corollary 1] and are summarised below, in a form adapted to the present context.

Theorem 2 (Dieker-Mandjes 2005) *Assume that, for some given ϑ^*,*

(V1) *$\{P_n\}$ satisfies an LDP with good rate function I,*
(V2) *$\limsup_{n\to\infty} \frac{1}{n}\log \varphi_n(\gamma n\vartheta^*) < \infty$ for some $\gamma > 1$, and, likewise, with ϑ^* replaced by $-\vartheta^*$,*
(V3) *The rare event A is both an I-continuity set and an $(I + \langle \vartheta^*, .\rangle)$-continuity set.*

Then, the tilted measure $\{P_n^{\vartheta^*}\}$ is asymptotically efficient for simulating A if and only if

$$\inf_{x\in\mathbb{R}^d}[I(x) - \langle \vartheta^*, x\rangle] + \inf_{x\in\overline{A}}[I(x) + \langle \vartheta^*, x\rangle] = 2\inf_{x\in A^\circ} I(x). \tag{19}$$

We use assumption (V2) here to replace the weaker but less easy to verify condition (2) in Assumption 1 of [9], in line with the paragraph below (2) in [9], or [7, Thm. 4.3.1]. Note also that (V2) holds automatically if $\varphi_n(n\vartheta)$ exists for all ϑ − but this is not mandatory here, since only a given ϑ^* is considered.

The proof of Theorem 2 is given in [9] and need not be recapitulated here; but we would like to comment briefly on what happens in the central condition (19). Replacing Q_n by $P_n^{\vartheta^*}$ in (16) and (15), we can rewrite η_N^2 as

$$\begin{aligned}
\eta_N^2(P_n^{\vartheta^*}, A) &= \frac{\mathbb{V}_{P_n^{\vartheta^*}}(\widehat{P_{P_n^{\vartheta^*}}(A)})_N}{(P_n(A))^2} = \frac{1}{N}\frac{\mathbb{V}_{P_n^{\vartheta^*}}(\widehat{P_{P_n^{\vartheta^*}}(A)})_1}{(P_n(A))^2} \\
&= \frac{1}{N}\frac{1}{(P_n(A))^2}\Big[\int_A \Big(\frac{\mathrm{d}P_n}{\mathrm{d}P_n^{\vartheta^*}}\Big)^2 \mathrm{d}P_n^{\vartheta^*} - (P_n(A))^2\Big].
\end{aligned} \tag{20}$$

Obviously (by (V1) and (V3)), $2\inf_{x\in A^\circ} I(x)$ (i.e., the right-hand side of (19)) is the exponential decay rate of $(P_n(A))^2$. Inspection of the proof of Theorem 2 reveals that the left-hand side of (19) is the exponential decay rate of $\int_A \Big(\frac{\mathrm{d}P_n}{\mathrm{d}P_n^{\vartheta^*}}\Big)^2 \mathrm{d}P_n^{\vartheta^*}$. It is clear from (20) that, for asymptotic efficiency to hold, $\int_A \Big(\frac{\mathrm{d}P_n}{\mathrm{d}P_n^{\vartheta^*}}\Big)^2 \mathrm{d}P_n^{\vartheta^*}$ must tend to zero at least as fast as $(P_n(A))^2$. But it cannot decrease faster, since $\mathbb{V}_{P_n^{\vartheta^*}}(\widehat{P_{P_n^{\vartheta^*}}(A)})_1$ is nonnegative, so that $\int_A \Big(\frac{\mathrm{d}P_n}{\mathrm{d}Q_n}\Big)^2 \mathrm{d}Q_n \geq (P_n(A))^2$ for arbitrary Q_n. Hence, the exponential decay rates must be exactly equal, as stated by (19). (A closely related argument is given in [5, Ch. 5.2].)

Theorem 2 is widely applicable. It holds in many standard situations, in particular in many of those that arise in applications.

Proposition 1 *Let $\{P_n\}$ be a family of probability measures that satisfy the conditions of the Gärtner-Ellis theorem, with (good) rate function I. Let A be a rare event with dominating point a, let ϑ^* be the unique solution of $\nabla\Lambda(\vartheta) = a$, and assume (V2) and (V3). Then $\{P_n^{\vartheta^*}\}$ is the unique tilted family that is asymptotically efficient for simulating $P_n(A)$.*

Proof The proof is a simple application of Thm. 2. (V1) follows from the Gärtner-Ellis theorem; we only need to verify condition (19). For the first infimum in (19), one obtains

$$\inf_{x \in \mathbb{R}^d}[I(x) - \langle \vartheta^*, x \rangle] = -\Lambda(\vartheta^*) = I(a) - \langle \vartheta^*, a \rangle. \tag{21}$$

Here, the first step follows from the convex duality lemma (compare [7, Lemma 4.5.8]), which is applicable since Λ is lower semicontinuous by (G3), and convex and $> -\infty$ everywhere (this follows from (G1) and (G2) by [8, Lemma V.4]). The second step is due to part b) of the dominating point property of a, together with Eq. (12).

As to the second infimum in (19), a minimises both I and $\langle \vartheta^*, . \rangle$ on A (by the dominating point property). Together with (V3), this gives

$$\inf_{x \in \overline{A}}[I(x) + \langle \vartheta^*, x \rangle] = I(a) + \langle \vartheta^*, a \rangle. \tag{22}$$

Eqs. (21) and (22) together give (19) because $\inf_{x \in A^\circ} I(x) = \inf_{x \in \partial A} I(x) = I(a)$. □

Remark 1 Note that an efficiency result closely related to Proposition 1 has previously been given by Bucklew [5, Thm. 5.2.1], but this is based on the variance rather than the relative error; and it is only a sufficient condition.

Note also that our assumption of a dominating point greatly simplifies the situation. Theorem 2 also allows to cope with situations without a dominating point – but this is not needed below.

Let us now apply this theory to the T-cell model.

4 Rare event simulation: the T-cell model

Recall that simulating the T-cell model means sampling the random variables $G(z^{(f)})$ of (3) and estimating the corresponding tail probabilities $\mathbb{P}(G(z^{(f)}) \geq g_{\text{act}})$. Inspection of Eq. (3) reveals two difficulties:

1. $G(z^{(f)})$ is a weighted sum of i.i.d. random variables, to which the standard results for sums of i.i.d. random variables (in particular, Cramér's theorem) are not applicable. We therefore need an extension to weighted sums – or, better, to general sums of independent, but not identically distributed random variables, which include weighted sums as a simple special case. This is straightforward and will be the subject of Sect. 4.1. In particular, it will be seen that, like in the i.i.d. case, every term in the sum must be tilted with the same parameter, but now this global tilting factor is a function of all the individual distributions involved.

2. Simulating the random variables $W_j = w(\mathcal{T}_j)$ is straightforward via simple sampling: draw $\text{Exp}(1/\bar{\tau})$ distributed random numbers τ_j (as realisations of $\mathcal{T}_j$) and apply the transformation (1). However, simulating the corresponding tilted variables is a difficult task, for two reasons. First of all, there is no indication of how to sample from the tilted distribution via transformation of one of the elementary distributions (like $\text{Uni}_{[0,1]}$ (the uniform distribution on the unit interval), or $\text{Exp}(\lambda)$) for which efficient random number generation is possible. Although such a transformation might exist in principle, there is no systematic way of finding it. One reason for this is that tilting acts at the level of the densities, but even the original (untilted) density of $W = w(\mathcal{T})$ is not available explicitly. (With W and $\mathcal{T}$ (without indices) we mean any representative of the family.) This is because its calculation requires the inverse functions and derivatives of the two branches (increasing and decreasing) of the function w, but these are unavailable analytically.

   In the absence of a transformation method, one might consider to determine the tilted density numerically, integrate it (again numerically) and discretise and tabulate the resulting distribution function. However, this is, again, forbidding for our particular function w: due to the vanishing derivatives at $\mathcal{T} = 0$ and $\mathcal{T} = 1$, the transformation formula for densities yields singularities in the density of W at these values, with a sizeable fraction of the probability

mass concentrated very close to 0 (see Fig. 3). This renders numerical calculations unreliable. To circumvent these problems, we will, in Sect. 4.2, present a sampling method for the tilted random variable W^ϑ that is based on tilting $\mathcal{T}$ rather than W itself.

4.1 Large deviations for independent but not identically distributed random variables

We consider K independent families of i.i.d. $\mathbb{R}^d$-valued random variables, $\{Y_\ell^{(1)}\}, \ldots, \{Y_\ell^{(K)}\}$ (i.e., the distribution within any given family $\{Y_\ell^{(k)}\}$, $1 \leq k \leq K$, is fixed, but the distributions may vary across families). Assume that $\Lambda^{(k)}(\vartheta) := \log \mathbb{E}(e^{\langle \vartheta, Y_1^{(k)} \rangle})$, the log moment-generating function of $Y_1^{(k)}$, is finite for all $\vartheta \in \mathbb{R}^d$ and $1 \leq k \leq K$ (here, $\mathbb{E}(.)$ refers to the probability measure induced by the random variable involved). Let $n^{(1)}, \ldots, n^{(K)}$ be positive integers, $n := \sum_{k=1}^K n^{(k)}$,

$$V_n := \sum_{\ell=1}^{n^{(1)}} Y_\ell^{(1)} + \ldots + \sum_{\ell=1}^{n^{(K)}} Y_\ell^{(K)}, \tag{23}$$

and P_n be the probability measure induced by $S_n = V_n/n$. In the limit $n \to \infty$, subject to $n^{(k)}/n \to \gamma^{(k)}$ for all $1 \leq k \leq K$, the limiting log-moment generating function of $\{S_n\}$ becomes

$$\Lambda(\vartheta) = \lim_{n \to \infty} \frac{1}{n} \log \mathbb{E}(e^{\langle \vartheta, V_n \rangle}) = \lim_{n \to \infty} \sum_{k=1}^K \frac{n^{(k)}}{n} \Lambda^{(k)}(\vartheta) = \sum_{k=1}^K \gamma^{(k)} \Lambda^{(k)}(\vartheta), \tag{24}$$

where the second step is due to independence. Since, by assumption, $\Lambda^{(k)}(\vartheta) < \infty$ for all $\vartheta \in \mathbb{R}^d$ and $1 \leq k \leq K$, the $\Lambda^{(k)}$ are differentiable on all of $\mathbb{R}^d$ (see [7, Lemma 2.2.31]); in fact, they are even $C^\infty(\mathbb{R}^d)$ [7, Ex.ercise 2.2.24]. Thus, Λ is $C^\infty(\mathbb{R}^d)$ as well.

By (24), we have (G1). Again due to $\Lambda^{(k)}(\vartheta) < \infty$, (G2) and (G5) are automatically satisfied. Furthermore, the differentiability of Λ entails (G3) and (G4). We have therefore shown

Lemma 1 *Under the assumptions of this paragraph, $\{P_n\}$ satisfies the Gärtner-Ellis theorem, with rate function I given by Eq. (10).* □

Such $\{P_n\}$ are therefore candidates for efficient simulation according to Prop. 1. The tilting factor ϑ^* may not be accessible analytically, but can be evaluated numerically from (11). Due to independence, tilting of S_n with $n\vartheta^*$ (that is, tilting of V_n with ϑ^*) is equivalent to tilting each $Y_\ell^{(k)}$ with ϑ^*.

4.2 Tilting of transformed random variables

Unlike the W_j, the $\text{Exp}(1/\bar{\tau})$-distributed random variables $\mathcal{T}_j$ are tilted easily (tilting with ϑ simply gives $\text{Exp}(-\vartheta + 1/\bar{\tau})$). One is therefore tempted to tilt the $\mathcal{T}_j$ rather than the W_j, or, in other words, to interchange the order of tilting and transformation. The following Theorem states the key idea.

Theorem 3 *Let X be an $\mathbb{R}^d$-valued random variable with probability measure μ, and let $Y := h \circ X$ (or $Y = h(X)$ by slight abuse of notation), where $h : \mathbb{R}^d \to \mathbb{R}^d$ is μ-measurable. Then Y has probability measure $\nu = \mu \circ h^{-1}$, where $h^{-1}(y)$ denotes the preimage of y. Assume now that $\mathbb{E}_\mu(e^{\langle \vartheta, h(X) \rangle})$ exists, let $\tilde{X}^\vartheta$ be an $\mathbb{R}^d$-valued random variable with probability measure $\tilde{\mu}^\vartheta$ related to μ via*

$$\frac{d\tilde{\mu}^\vartheta}{d\mu}(x) = \frac{e^{\langle \vartheta, h(x) \rangle}}{\mathbb{E}_\mu(e^{\langle \vartheta, h(X) \rangle})} \tag{25}$$

(so that $\tilde{\mu}^\vartheta \ll \mu$), and let $\tilde{Y}^\vartheta = h(\tilde{X}^\vartheta)$. Then, the measures $\tilde{\nu}^\vartheta$ (of $\tilde{Y}^\vartheta$) and ν^ϑ (for the tilted version of ν, belonging to Y^ϑ) are equal, where $\nu^\vartheta \ll \nu$ with Radon-Nikodym density

$$\frac{\mathrm{d}\nu^\vartheta}{\mathrm{d}\nu}(y) = \frac{e^{\langle\vartheta,y\rangle}}{\mathbb{E}_\nu(e^{\langle\vartheta,Y\rangle})}. \tag{26}$$

Proof Note first that $e^{\langle\vartheta,y\rangle}$ is clearly μ-measurable, and

$$\mathbb{E}_\nu(e^{\langle\vartheta,Y\rangle}) = \int_{\mathbb{R}^d} e^{\langle\vartheta,y\rangle}\mathrm{d}\nu(y) = \int_{\mathbb{R}^d} e^{\langle\vartheta,h(x)\rangle}\mathrm{d}\mu(x) = \mathbb{E}_\mu(e^{\langle\vartheta,h(X)\rangle}), \tag{27}$$

which exists by assumption, so ν^ϑ is well-defined. We now have to show that $\tilde{\nu}^\vartheta(B) = \nu^\vartheta(B)$ for arbitrary Borel sets B. Observing that $\tilde{\nu}^\vartheta = \tilde{\mu}^\vartheta \circ h^{-1}$ and employing the formulas for transformation of measures [3, (13.7)] and change of variable [3, Thm. 16.13], together with (25), one indeed obtains

$$\begin{aligned}
\tilde{\nu}^\vartheta(B) &= \tilde{\mu}^\vartheta\big(h^{-1}(B)\big) = \int_{h^{-1}(B)} \frac{\mathrm{d}\tilde{\mu}^\vartheta}{\mathrm{d}\mu}(x)\mathrm{d}\mu(x) = \frac{1}{\mathbb{E}_\mu(e^{\langle\vartheta,h(X)\rangle})} \int_{h^{-1}(B)} e^{\langle\vartheta,h(x)\rangle}\mathrm{d}\mu(x) \\
&= \frac{1}{\mathbb{E}_\nu(e^{\langle\vartheta,Y\rangle})} \int_B e^{\langle\vartheta,y\rangle}\mathrm{d}\nu(y) = \int_B \frac{\mathrm{d}\nu^\vartheta}{\mathrm{d}\nu}(y)\mathrm{d}\nu(y) = \nu^\vartheta(B),
\end{aligned} \tag{28}$$

which proves the claim. □

In words, Theorem 3 is nothing but the simple observation that, to obtain the tilted version of $Y = h(X)$, one can reweight the measure μ of X with the factors $e^{\langle\vartheta,h(x)\rangle}$, rather than reweighting the measure ν of Y with $e^{\langle\vartheta,y\rangle}$. It should be clear, however, that the measure $\tilde{\mu}^\vartheta$ differs from the usual tilted version of μ, which would involve tilting factors $e^{\langle\vartheta,x\rangle}$ rather than $e^{\langle\vartheta,h(x)\rangle}$; for this reason, we use the notation $\tilde{\mu}^\vartheta$ rather than μ^ϑ. Such kind of tilting is common in large deviation theory (see, e.g., [7, Chap. 2.1.2]). Nevertheless, the simple observation above is the key to simulation if μ (and $\tilde{\mu}^\vartheta$) are readily accessible at least numerically, but ν (and ν^ϑ) are not.

This is precisely our situation, with $\tilde{\mathcal{T}}^\vartheta$, αW^ϑ and αw ($\alpha \in \{qz^{(c)}, qz^{(v)}, z^{(f)}\}$), respectively, taking the roles of $\tilde{X}^\vartheta$, Y^ϑ and h (we will use f, $\tilde{f}^\vartheta$, g and g^ϑ for the corresponding densities of $\mathcal{T}$, $\tilde{\mathcal{T}}^\vartheta$, αW, and $(\alpha W)^\vartheta$). Still, reweighting of the exponential density of $\mathcal{T}$ with $e^{\vartheta\alpha w(\tau)}$ does not yield an explicit closed-form density, and no direct simulation method is available for the corresponding random variables. However, the reweighted densities are easily accessible numerically, in contrast to those of W and its tilted variant, W^ϑ. The problem may thus be solved by calculating and integrating $\tilde{f}^\vartheta$ numerically and discretising and tabulating the resulting distribution function $\tilde{F}^\vartheta$. Samples of $\tilde{\mathcal{T}}^\vartheta$ may then be drawn according to this table (i.e., by formally looking up the solution of $\tilde{F}(\tilde{\mathcal{T}}^\vartheta) = U$ for $U \sim \mathrm{Uni}_{[0,1]}$), and $\alpha W^\vartheta = \alpha w(\tilde{\mathcal{T}}^\vartheta)$ is then readily evaluated. The only difficulty left is the time required for searching the table. But this is a practical matter and will be dealt with in the next paragraph.

4.3 The algorithm

Taking together our theoretical results, we can now detail the specific importance sampling algorithm for the simulation of the T-cell model of Sect. 2. If not stated otherwise, we will refer to the basic model (3). Recall that it describes the stimulation rate $G(z^{(f)})$ and we wish to evaluate the probability $\mathbb{P}(G(z^{(f)}) \geq g_{\text{act}})$.

To apply LD sampling, let us embed the model into a sequence of models with increasing total number $n = n^{(c)} + n^{(v)} + n^{(f)}$ of antigen types, where $n^{(c)}$, $n^{(v)}$, and $n^{(f)}$ are the numbers of constitutive, variable and foreign antigen types. (This is an aritificial sequence of models required

to formulate the limiting process involved in the theory; in contrast to the original model, there can now be multiple foreign antigen types.) Let

$$G_n(z^{(f)}) = \left(\sum_{j=1}^{n^{(c)}} q_n z^{(c)} W_j \right) + \left(\sum_{j=n^{(c)}+1}^{n^{(c)}+n^{(v)}} q_n z^{(v)} W_j \right) + \left(\sum_{j=n^{(c)}+n^{(v)}+1}^{n^{(c)}+n^{(v)}+n^{(f)}} z^{(f)} W_{n^{(c)}+n^{(v)}+j} \right), \quad (29)$$

where

$$q_n = \frac{n^{(c)} z^{(c)} + n^{(v)} z^{(v)} - n^{(f)} z^{(f)}}{n^{(c)} z^{(c)} + n^{(v)} z^{(v)}} \quad (30)$$

(where $z^{(c)}$, $z^{(v)}$, and $z^{(f)}$ are independent of n). Clearly, $G_n(z^{(f)})$ coincides with $G(z^{(f)})$ of (3) if $n^{(c)} = m^{(c)}$, $n^{(v)} = m^{(v)}$, and $n^{(f)} = m^{(f)}$, where $m^{(f)} = 0$ or $m^{(f)} = 1$ depending on whether $z^{(f)} = 0$ or $z^{(f)} > 0$; then, $n = m = m^{(c)} + m^{(v)} + m^{(f)}$. We have to consider $\mathbb{P}\big(G_n(z^{(f)})/n > g_{\mathrm{act}}/m\big)$ (this reflects the fact that g_{act} must scale with system size). The sequences $\{G_n(z^{(f)})\}$ and $\{G_n(z^{(f)})\}/n$ take the roles of $\{V_n\}$ and $\{S_n\}$, respectively, in Secs. 3.1 and 4.1, with P_n the law of $G_n(z^{(f)})/n$; and we consider $A = [g_{\mathrm{act}}/m, \infty)$ with $\mathbb{E}(G_m(z^{(f)})/m) < g_{\mathrm{act}}/m < Mw(1)/m$ (the latter is the maximum value of $G_m(z^{(f)})/m$ since $w(\tau)$ has its maximum at $\tau = 1$). The limit $n \to \infty$ is then taken so that $\lim_{n\to\infty} n^{(c)}/n = m^{(c)}/m$, $\lim_{n\to\infty} n^{(v)}/n = m^{(v)}/m$, as well as $\lim_{n\to\infty} n^{(f)}/n = m^{(f)}/m$, that is, the relative amounts of constitutive, variable, and foreign antigens approach those fixed in the original model, (3). (Note that, in [37], a different limit was employed, namely, $n \to \infty$ with $\lim_{n\to\infty} n^{(c)}/n^{(v)} = C_1 \in (0, \infty)$ and $\lim_{n\to\infty} n^{(f)}/n = 0$; this is appropriate for exact asymptotics, but not for simulation, because the asymptotic tilting factor to be used in the latter then does not feel the foreign antigens.)

Lemma 2 *Let f be the density of $\mathrm{Exp}(1/\overline{\tau})$ (i.e., $f(\tau) = e^{-\tau/\overline{\tau}}/\overline{\tau}$), and*

$$\psi(t) := \mathbb{E}(e^{tW}) = \int_0^\infty \exp\big(tw(\tau)\big) f(\tau) d\tau = \frac{1}{\overline{\tau}} \int_0^\infty \exp\left(t\frac{\exp(-1/\tau)}{\tau} - \frac{\tau}{\overline{\tau}} \right) d\tau \quad (31)$$

be the moment-generating function of W_1. Under the assumptions of Sect. 4.3, the unique solution ϑ^* of

$$\begin{aligned}
\frac{g_{\mathrm{act}}}{m} = &\frac{m^{(c)}}{m} q z^{(c)} \left[\frac{\mathrm{d}}{\mathrm{d}t} \log \psi(t) \right]\Bigg|_{t=qz^{(c)}\vartheta} + \frac{m^{(v)}}{m} q z^{(v)} \left[\frac{\mathrm{d}}{\mathrm{d}t} \log \psi(t) \right]\Bigg|_{t=qz^{(v)}\vartheta} \\
&+ \frac{1}{m} z^{(f)} \left[\frac{\mathrm{d}}{\mathrm{d}t} \log \psi(t) \right]\Bigg|_{t=z^{(f)}\vartheta}
\end{aligned} \quad (32)$$

is the unique asymptotically efficient tilting parameter for LD simulation of $P_n(A)$.

Proof Clearly, P_n satisfies the assumptions of Sect. 4.1. Note, in particular, that $\psi(t) < \infty$ for all $t \in \mathbb{R}$ since W is bounded above and below, and so

$$\Lambda(\vartheta) = \lim_{n\to\infty} \log \mathbb{E}(e^{\vartheta G_n(z^{(f)})/n}) = \frac{m^{(c)}}{m} \log \psi(qz^{(c)}\vartheta) + \frac{m^{(v)}}{m} \log \psi(qz^{(v)}\vartheta) + \frac{1}{m} \log \psi(z^{(f)}\vartheta) < \infty \quad (33)$$

for all ϑ; hence, the Gärtner-Ellis theorem holds by Lemma 1. To verify the remaining assumptions of Prop. 1, recall from Sec. 4.1 that $\Lambda(\vartheta)$ is differentiable (with continuous derivative) on all of $\mathbb{R}$. The bounds on g_{act}/m lead to

$$\Lambda'(0) = \frac{\mathbb{E}\big(G(z^{(f)})\big)}{m} < \frac{g_{\mathrm{act}}}{m} < \frac{Mw(1)}{m} = \lim_{\vartheta\to\infty} \Lambda'(\vartheta). \quad (34)$$

Λ is strictly convex (since $(\mathrm{d}^2/\mathrm{d}t^2) \log \psi(t)$ is the variance of W^t, the tilted version of W (cf. [2, Prop. XII.1.1]), which is positive since W and hence W^t is nondegenerate). Eq. (34) thus entails that $\Lambda'(\vartheta) = g_{\mathrm{act}}/m$ has a unique solution ϑ^*, which is positive (and clearly satisfies (V2)). As a

consequence, g_{act}/m is a dominating point of A, which is a rare event since $0 < I(g_{\mathrm{act}}/m) < \infty$ (by $\Lambda(0) = 0$ together with (34) and (12); cf. Fig. 4, left). Finally, A is a continuity set of both I and $I + \langle \vartheta^*, . \rangle$ simply because I and $\langle \vartheta^*, . \rangle$ are continuous at g_{act}/m, and $A = \overline{A^\circ}$. Realising that the right-hand side of (32) equals $\Lambda'(\vartheta)$ (see also Eq. (20) in [37]), one obtains the claim from Prop. 1. □
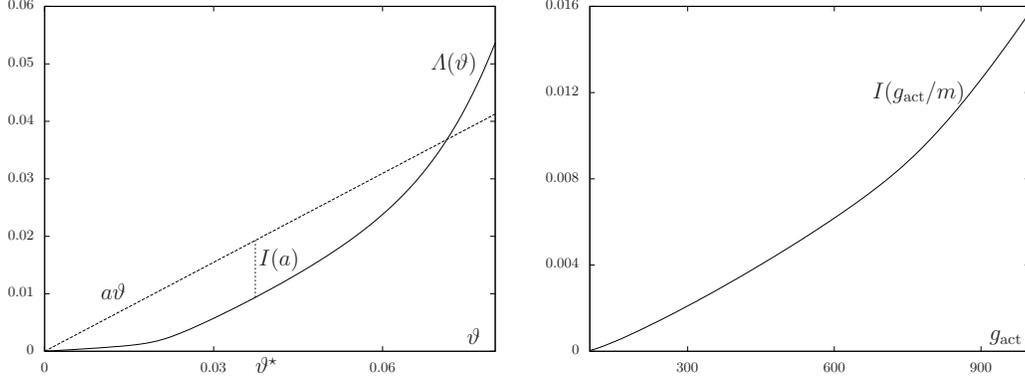
Fig. 4 The cumulant-generating function Λ (left) and the rate function I (right) for the T-cell model (3). The slope of the straight line in the left panel is $a = g_{\mathrm{act}}/m$, where $g_{\mathrm{act}} = 800$ and $m = 1551$. At ϑ^*, $a\vartheta - \Lambda(\vartheta)$ assumes its maximum, $I(a)$ (cf. (10) –(12)).

The solution of (32) is readily calculated numerically. The function Λ, and the resulting rate function I, are shown in Fig. 4.

As described in Sect. 4.2, we now tilt the density f of the $\mathcal{T}_j$ with ϑ^* according to Eq. (25). This yields three different densities $\tilde{f}_\alpha^{\vartheta^*}$, depending on the weighting factors $\alpha \in \{qz^{(c)}, qz^{(v)}, z^{(f)}\}$, namely

$$\tilde{f}_\alpha^{\vartheta^*}(\tau) = \frac{\exp(\alpha\vartheta^* w(\tau)) f(\tau)}{\psi(\alpha\vartheta^*)} = \frac{\frac{1}{\tau}\exp\left(\alpha\vartheta^* \frac{\exp(-1/\tau)}{\tau} - \frac{\tau}{\tau}\right)}{\psi(\alpha\vartheta^*)}. \tag{35}$$

As discussed in Sect. 4.2, this is not the density of any known standard distribution (let alone an exponential one), and simulating from it requires numerical integration (which is well-behaved since the $\tilde{f}_\alpha^{\vartheta^*}$ are numerically well-behaved), and discretisation and tabulation of the resulting distribution functions $\tilde{F}_\alpha^{\vartheta^*}$, followed by looking up the solution $\tilde{\tau}^{\vartheta^*}$ of $\tilde{F}_\alpha^{\vartheta^*}(\tilde{\mathcal{T}}^{\vartheta^*}) = U$ for $U \sim$ $\mathrm{Uni}_{[0,1]}$, to finally yield αW^{ϑ^*} via $\alpha W^{\vartheta^*} = \alpha w(\tilde{\mathcal{T}}^{\vartheta^*})$.

Searching the table would be the speed- (or precision-) limiting step, requiring $\mathcal{O}(\log D)$ operations if D is the number of discretisation steps. This can be remedied by applying the so-called *alias method* to quickly generate random variables according to the discretised probability distribution. For a description of the method, we refer the reader to [19, pp. 25–27], [16], or [24, p. 248]. Let us just summarise here that, after a preprocessing step, which is done once for a given distribution, the method only requires one $\mathrm{Uni}_{[0,1]}$ random variable together with one multiplication, one cutoff and one subtraction (or two $\mathrm{Uni}_{[0,1]}$ random variables together with one multiplication, one cutoff and one comparison, depending on the implementation) to generate one realisation of $\tilde{\mathcal{T}}^{\vartheta^*}$, regardless of D (in particular, it does without searching altogether).

We now have everything at hand to formulate the algorithm to simulate (realisations of) $G(z^{(f)})$ of (3). (For notational convenience, we will not distinguish between random variables and their realisations here).

Algorithm 1
compute ϑ^* by solving Eq. (32) numerically

calculate the tilted densities $\tilde{f}_\alpha^{\vartheta^*}$, $\alpha \in \{qz^{(c)}, qz^{(v)}, z^{(f)}\}$, *via* (35)

for *i=1 till sample size N* **do**

   for every summand j of (3) *generate a sample* $(\tilde{\mathcal{T}}_j^{\vartheta^*})^{(i)}$ *according to its density* $\tilde{f}_{\alpha(j)}^{\vartheta^*}$ *with the help of the alias method (here, the upper index* (i) *is added to reflect sample i, and* $\alpha(j)$ *is the weighting factor of the sum to which j belongs)*

   calculate

$$\left(G(z^{(f)})\right)^{(i)} = \left(\sum_{j=1}^{m^{(c)}} qz^{(c)}w\big((\tilde{\mathcal{T}}_j^{\vartheta^*})^{(i)}\big)\right) + \left(\sum_{j=m^{(c)}+1}^{m^{(c)}+m^{(v)}} qz^{(v)}w\big((\tilde{\mathcal{T}}_j^{\vartheta^*})^{(i)}\big)\right) + z^{(f)}w\big((\tilde{\mathcal{T}}_{m^{(c)}+m^{(v)}+1}^{\vartheta^*})^{(i)}\big)$$

   calculate the indicator function times the reweighting factor (i.e., the i-th summand in Eq. (15)*)*

if $(G(z^{(f)}))^{(i)} \geq g_{\mathrm{act}}$ **then**

$$R^{(i)} = \prod_{j=1}^{m} \frac{f_{\alpha(j)}((\tilde{\mathcal{T}}_j^{\vartheta^*})^{(i)})}{\tilde{f}_{\alpha(j)}^{\vartheta^*}((\tilde{\mathcal{T}}_j^{\vartheta^*})^{(i)})}$$

else

   $R^{(i)} = 0$

end if

end for

calculate $\left(\widehat{P_{P_m}^{\vartheta^*}(A)}\right)_N = \dfrac{\sum_{i=1}^{N} R^{(i)}}{N}$, *as estimate of* $\mathbb{P}(G(z^{(f)}) > g_{\mathrm{act}})$.

4.4 Extension to variable copy numbers

Let us now consider the extended model (4), in which the copy numbers are themselves random variables. This is also covered by the large deviation theory presented above; in particular, Lemma 1 again applies if the $Y_\ell^{(k)}$ in (23) are identified with $Z_j^{(c)}W_j$ or $Z_j^{(v)}W_j$, respectively. The global tilting factor ϑ^* is, in the usual way, calculated as the solution of $\Lambda'(\vartheta) = g_{\mathrm{act}}/m$, where $\Lambda(\vartheta)$ is as in (33) with $\psi(qz^{(k)}\vartheta) = \mathbb{E}(e^{qz^{(k)}\vartheta W})$ replaced by $\mathbb{E}(\psi(qZ^{(k)}\vartheta)) = \mathbb{E}(e^{qZ^{(k)}\vartheta W})$, $k \in \{c, v\}$; see Eq. (20) in [37].

However, the object of tilting now is the *joint distribution* of W and $Z^{(c)}$ (or $Z^{(v)}$, respectively), that is, $\mathrm{d}F(\tau)\mathrm{d}H^{(k)}(z)$ receives the reweighting factor $\exp(q\vartheta zw(\tau))$, where F and $H^{(k)}$ denote the measures of $\mathcal{T}$ and $Z^{(k)}$, $k \in \{c, v\}$, respectively. This introduces dependencies between copy numbers and stimulation rates. The resulting *bivariate* simulation task is costly and may offset some of the efficiency gain obtained by tilting.

If, however, the $Z^{(k)}$ are closely peaked around their means (as is the case for our choice of parameters), the following hybrid procedure turns out to be both practical and fast: Draw the $Z^{(k)}$ from their original (untilted, binomial) distributions; and simulate a tilted version of qW, denoted by $(\overline{qW})^{\vartheta^*}$, by reweighting the original density of qW with $\exp(q\vartheta^*\mathbb{E}(Z^{(k)})W)$, irrespective of the actual value of Z. Clearly, this method is not asymptotically efficient, but it is a valid importance sampling method that turns out to compare well with the ideal procedure used for the fixed copy numbers (see Sec. 5.1.3).

5 Results

Let us now present the results of our simulations in two steps. We first investigate the performance of the method, and then use it to gain more insight into the underlying phenomenon of statistical recognition.

5.1 Performance of the simulation method

We will examine the performance of the importance-sampling method in three respects: we will compare it to simple sampling (the previously-used simulation method) and to the results of exact asymptotics (the previously-used analytic method); finally, we will quantify the efficiency in terms of the relative error (and thus return to the theory of Sect. 3.2). In any case, we will consider $\mathbb{P}(G(z^{(f)}) \geq g_{\text{act}})$ as a function of g_{act} (and for various values of the parameter $z^{(f)}$). Of course, this probability is just one minus the distribution function of $G(z^{(f)})$; in immunobiology, the corresponding graph is known as the activation curve.

Evaluating this graph by LD simulation requires, for each value of g_{act} to be considered, a fresh sample, simulated with its individual tilting factor ϑ^* (recall that this depends on g_{act} via (32)). At first sight, this looks like an enormous disadvantage relative to simple sampling, where no threshold needs to be specified in advance; rather, the outcomes of the simulation directly yield an estimate over the entire range of the activation curve. However, it will turn out that this disadvantage is offset many times by the specific efficiency of hitting the rare events in LD sampling. (There is room for improvement: the samples that do not hit a given rare event could be used to improve the estimates of the more likely events.)

5.1.1 Comparison with simple sampling

Clearly, both the simple-sampling and the importance-sampling estimates are unbiased and converge to the true values as $N \to \infty$. It is therefore no surprise that they yield practically identical results wherever they can be compared – and this yields a first quick consistency check for our method.

This is demonstrated in Fig. 5, which shows simple sampling (SS) and importance sampling (IS) activation curves, each for $z^{(f)} = 1000$ and $z^{(f)} = 2000$. For SS, $N = 1.3 * 10^8$ samples, $(G(z^{(f)}))^{(i)}, 1 \leq i \leq N$, were generated altogether for every graph, whereas for IS, $N = 10000$ samples were generated for every threshold value considered (from $g_{\text{act}} = 100$ to $g_{\text{act}} = 1000$ in steps of 50), i.e. $1.9 * 10^5$ samples altogether. Beyond $g_{\text{act}} = 450$ and $g_{\text{act}} = 800$ (for $z^{(f)} = 1000$ and $z^{(f)} = 2000$, respectively), no estimates could be obtained via SS due to the low probabilities involved, whereas with IS, it is easy to get beyond $g_{\text{act}} = 900$ in either case, although the probabilities can get down to 10^{-20} (note, however, that this far end of the distribution is no longer biologically relevant). In terms of runtime, determining an activation curve (over its entire range) by SS took 48 hours of CPU time (Intel Pentium M 1.4 GHz 512MB RAM), whereas IS required only about 2 minutes (in the threshold regime where the methods are comparable), that is, a speedup by a factor of nearly 1500 is achieved.

We also applied our method to the extended model (4) with binomially distributed copy numbers. Figure 6 shows the simulation results for two values of $z^{(f)}$, each for SS and IS. Again, the curves agree, as they must. As to runtime, it took about 130 hours to generate the $2 * 10^7$ samples for SS, whereas for IS it took 10 min. to generate the $9.5 * 10^4$ samples.

5.1.2 Comparison with exact asymptotics

A pillar of the previous analysis of Zint et al. [37] (and its precursor BRB [33]) has been so-called exact asymptotics. This is a refinement of large deviation theory which yields estimates for the probabilities $P_n(A)$ themselves, rather than just their exponential decay rates obtained via the LDP in Def. 1. With standard large deviation theory (and our simulation method), it shares the tilting parameter which is calculated according to Eq. (32); for more details, we refer to [37]. A comparison of IS simulation with exact asymptotics is also included in Fig. 5. For small values of g_{act}, exact asymptotics is slightly imprecise. This is due to the asymptotic nature ($n \to \infty$) of the method, which yields more precise results in the very tail of the distribution, where the deviations are truly large. Note that, although our tilting factors agree with those in exact asymptotics, rare event simulation does not suffer from this accuracy problem since, due to the reweighting, it is
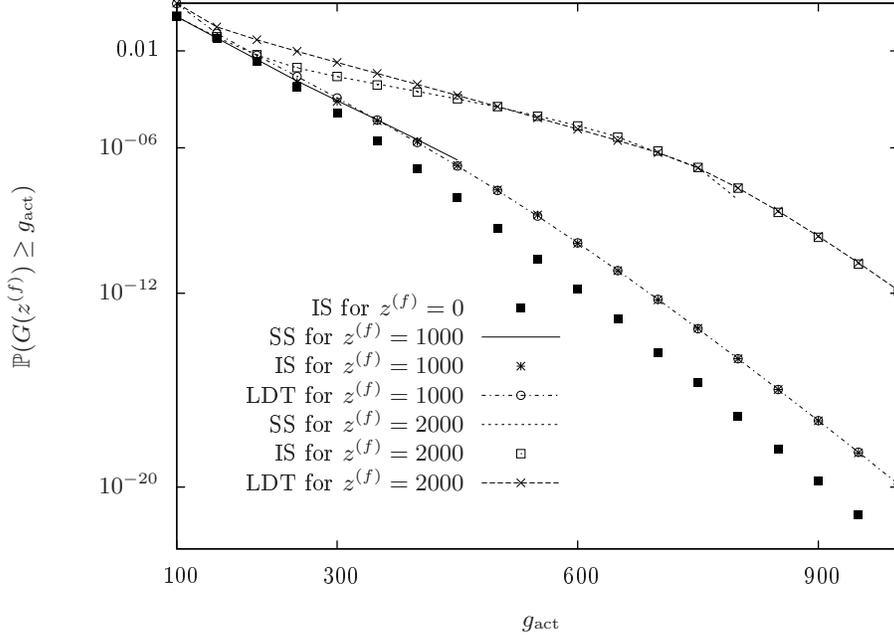
Fig. 5 Estimates of the activation curve, $\mathbb{P}(G(z^{(f)}) \geq g_{\text{act}})$, in the basic model (3) for $z^{(f)} = 1000$ and $z^{(f)} = 2000$, as well as for the self background ($z^{(f)} = 0$), on logarithmic scale. The probabilities were estimated independently with simple sampling (SS), importance sampling (IS), and exact asymptotics based on large deviation theory (LDT) as used in [37]. For IS, 19 values of g_{act} were considered (from 100 to 1000 in steps of 50), and $N = 10000$ samples were generated for each value (i.e., $1.9 * 10^5$ samples altogether), whereas for the SS simulation, $N = 1.3 * 10^8$ samples were used over the entire range. The SS curves end at $g_{\text{act}} = 400$ and $g_{\text{act}} = 800$, respectively, because larger values were not hit in the given sample. The IS and SS graphs agree perfectly until the SS simulation lacks precision. For larger threshold values, we see a perfect agreement of the IS and LDT graphs. Note the general feature that, for threshold values that are not too small, the activation probability in the presence of foreign antigens is several orders of magnitude larger than the self background, i.e. Eq. (6) is satisfied.

always a valid importance sampling scheme that yields unbiased estimates for every finite n; the finite-size effects will only manifest themselves as a certain loss of efficiency, as will be seen below.

5.1.3 Asymptotic efficiency and relative error

In order to investigate the relative error of $(\widehat{P_{P_n^{\vartheta*}}(A)})_N$, we first note that the variance of the estimator is given by

$$\mathbb{V}\left(\left(\widehat{P_{P_n^{\vartheta*}}(A)}\right)_N\right) = \frac{1}{N}\mathbb{V}\left(\left(\widehat{P_{P_n^{\vartheta*}}(A)}\right)_1\right) = \frac{1}{N}\mathbb{E}\left[\left(\mathbb{1}\{(T_n^{\vartheta*})^{(1)} \in A\}\frac{\mathrm{d}P}{\mathrm{d}P_n^{\vartheta*}}((T_n^{\vartheta*})^{(1)}) - P_n(A)\right)^2\right],$$
(36)

where we have used (15) for $N = 1$. $\mathbb{V}\left(\left(\widehat{P_{P_n^{\vartheta*}}(A)}\right)_1\right)$ can be estimated via the given number N of samples in a single simulation run, i.e., as the sample variance

$$\widehat{\mathbb{V}}\left(\left(\widehat{P_{P_n^{\vartheta*}}(A)}\right)_1\right) = \frac{1}{N-1}\sum_{i=1}^{N}\left(\mathbb{1}\{(t_n^{\vartheta*})^{(i)} \in A\}\frac{\mathrm{d}P}{\mathrm{d}P_n^{\vartheta*}}((t_n^{\vartheta*})^{(i)}) - \left(\widehat{P_{P_n^{\vartheta*}}(A)}\right)_N\right)^2, \qquad (37)$$
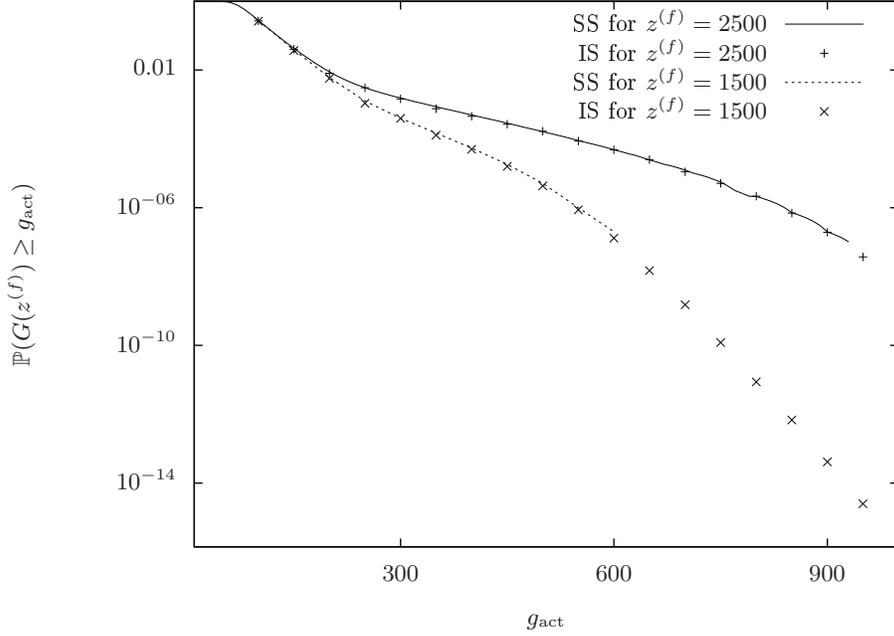
Fig. 6 Simulation of $\mathbb{P}(G(z^{(f)}) \geq g_{\text{act}})$ in the extended model (4), for $z^{(f)} = 1500$ and $z^{(f)} = 2500$. The probabilities were estimated independently with simple sampling, and with importance sampling at 19 different threshold values (from 100 to 1000 in steps of 50). For IS, $9.5 * 10^4$ samples were generated (5000 per threshold); for SS, $2 * 10^7$ samples were used. No estimates are obtained with SS at thresholds beyond 600 or 920, respectively, in analogy with the situation in Fig. 5.

where the $(t_n^{\vartheta^*})^{(i)}$ are now considered as realisations of $(T_n^{\vartheta^*})^{(1)}$. We can thus estimate the squared relative error as

$$\widehat{\eta_N^2}(P_n^{\vartheta^*}, A) = \frac{1}{N} \frac{\widehat{\mathbb{V}}\left(\widehat{(P_{P_n^{\vartheta^*}}(A))_1}\right)}{\left(\widehat{(P_{P_n^{\vartheta^*}}(A))_N}\right)^2}. \tag{38}$$

For simple sampling, one proceeds in the obvious analogous way (without tilting and reweighting).

In line with the limit discussed in Sec. 4.3, we now consider $G_n(z^{(f)})$ for system sizes $n = n_i$, where $n_i = n_i^{(c)} + n_i^{(v)} + n_i^{(f)}$, $0 \leq i \leq 10$, and we choose $n_i^{(\alpha)} = im^{(\alpha)}$, $\alpha \in \{c, v, f\}$, for $1 \leq i \leq 10$, as well as $n_0^{(c)} = m^{(c)}/2$, $n_0^{(v)} = m^{(v)}/2$, and $n_0^{(f)} = m^{(f)}$ (i.e., we simply 'multiply' the system, except for $i = 0$, which corresponds to 'half' a system except for the foreign peptide, which cannot be split into two). We then simulate $\mathbb{P}(G_{n_i}(z^{(f)}) \geq g_{\text{act}} n_i/m)$ for two values of $z^{(f)}$ and a fixed value of g_{act} with our importance sampling method, as shown in Fig. 7.

Obviously, the (estimated) probabilities decay to zero at an exponential rate with increasing n, as they must by their LDP. In contrast, the (estimated) squared RE only increases linearly – this even goes beyond the prediction of the theory (asymptotic efficiency only guarantees a subexponential increase).

So far, we have considered the n-dependence of the method for a fixed value of g_{act}, in the light of the available asymptotic theory. For the practical simulation of the given T-cell problem, we now take the given system size $n = m$ and numerically investigate the relative error as a function of g_{act}. Here, the exponential decay of $\mathbb{P}(G(z^{(f)}) \geq g_{\text{act}})$ as a function of g_{act} is decisive, which we have already observed in Fig. 5, and which goes together with the at-least-linear *increase* of I with g_{act} (recall that I is convex, and see Fig. 4). Fig. 8 shows the relative error of both SS and IS. It does not come as a surprise that, again, IS does extremely well and beats the exponential
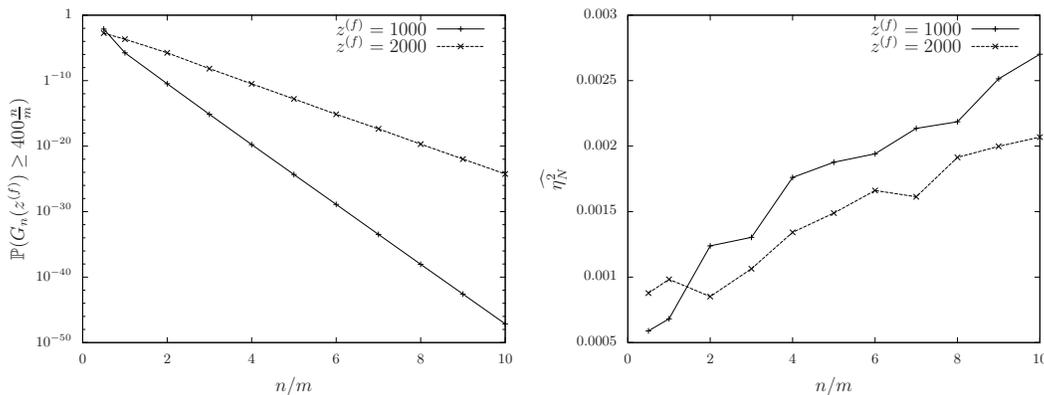
Fig. 7 Importance sampling simulations for $\mathbb{P}(G_n(z^{(f)}) \geq g_{\mathrm{act}} n/m)$ for $n = n_i$, $0 \leq i \leq 10$, for $g_{\mathrm{act}} = 400$ and two values of $z^{(f)}$. Left: estimate of the probability (note that the vertical axis is on logarithmic scale). Right: estimated squared RE.

decay of the probabilities: whereas, on the log scale of the vertical axis, the squared RE of SS grows roughly linearly, it remains more or less constant for IS. (The very low squared RE of the simple sampling graphs for low thresholds in the right panel is due to the fact that the probability to reach this threshold is quite high and the huge sample of $N = 1.3 \cdot 10^8$ contributes to estimating it, that is, the sample sizes are not comparable. A simple sampling simulation run with the total sample size of a corresponding IS simulation (i.e., $N = 10000$ times the number of steps contained in the interval considered) results in higher relative errors than for importance sampling even for the low threshold values (left panel). We would like to note, however, that the runtime of simple sampling for these small sample sizes is shorter than the runtime for IS, even if one does not count the overhead required to get the tilting parameters for importance sampling.)
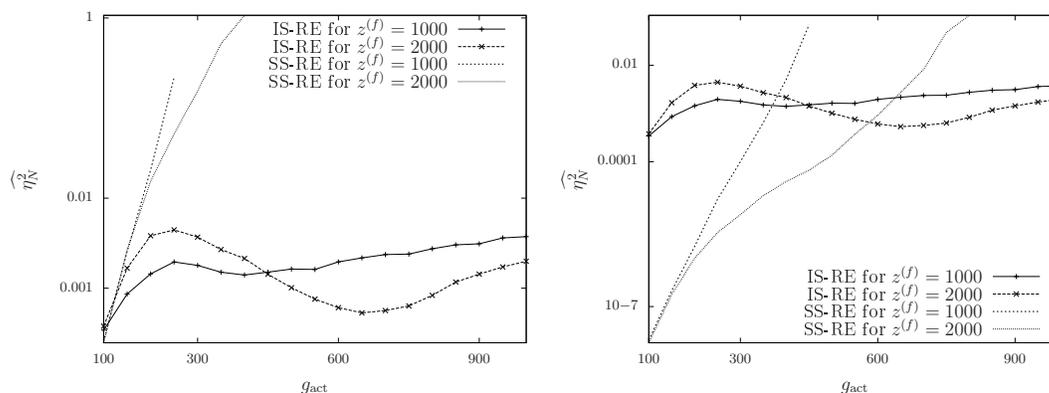

Fig. 8 Estimated squared RE for simple sampling ($N = 10000$ times the number of steps contained in the considered interval (left), $N = 1.3 * 10^8$ (right)), and importance sampling ($N = 10000$ per threshold value in either panel) simulations of $\mathbb{P}(G(z^{(f)}) > g_{\mathrm{act}})$ of the basic model, Eq. (3). Note that the vertical axis is on logarithmic scale.

Figure 9 sheds more light on the behaviour of the relative error of the IS simulation. It shows the squared RE for 6 distinct $z^{(f)}$-values and reveals the finite-size effects. The wave-like behaviour for larger $z^{(f)}$ is due to the fact that, for very low threshold values, there is no real need for tilting, because the original distribution P_n is already close to optimal and the tilting factor is very small. For increasing thresholds, substantial tilting is required, but there are still visible deviations from
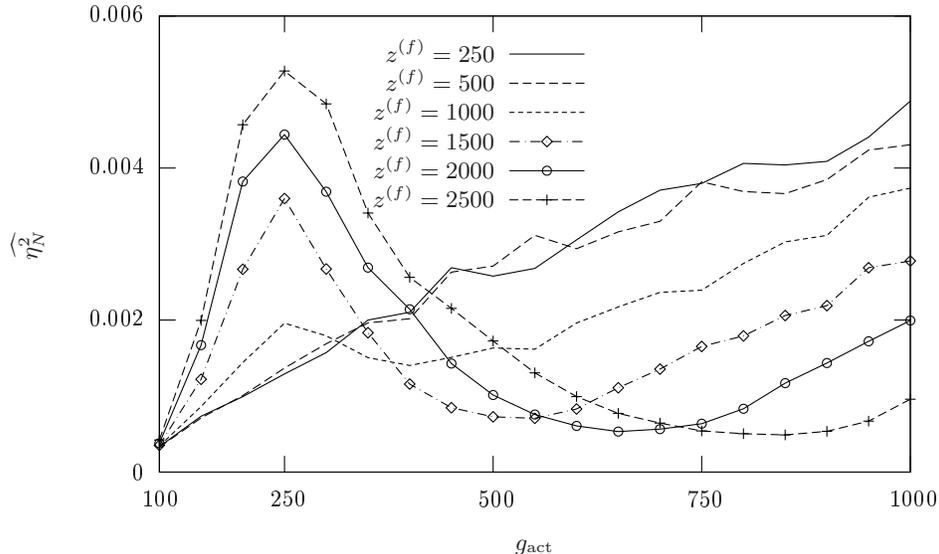
Fig. 9 Estimated squared RE of our IS estimate, for various frequencies $z^{(f)}$ of the foreign antigen. Details are as in Fig. 8, but now the vertical axis is on linear scale.

the $n \to \infty$ limit (as already discussed in the context of Fig. 5), so the tilted distributions are not optimal. This produces the hump in the squared RE curves, which is more pronounced for larger $z^{(f)}$ values because, for the case $n = m$ considered here, the foreign antigens come as a single term that may stand out. For large g_{act}, finally, one gets close enough to the limit, and the expected sub-exponential increase sets in (in our case, it is, in fact, roughly linear). Nevertheless, it should be clear that, in spite of the slight non-optimality at small threshold values, our tilted distributions still yield a far lower squared RE than does simple sampling. A very similar picture emerges for the extended model; surprisingly, the relative error is no larger than in the basic model, although the *ad hoc* simulation method used here is not asymptotically efficient (see Sec. 4.4; data not shown).

5.2 Analysis of the T-cell model

In this Section, we use our simulation method to obtain more detailed insight into the phenomenon of statistical recognition in the T-cell model. As discussed before, the task is to discriminate one foreign antigen type against a noisy background of a large number of self antigens. We already know from Fig. 5 that, for threshold values that are not too small, the activation probability in the presence of foreign antigens is several orders of magnitude larger than the activation probability of the self-background, i.e. Eq. (6) is satisfied. As discussed in [37], this distinction relies on $z^{(f)} > z^{(c)}, z^{(v)}$ – what happens is that larger copy numbers of the foreign antigen thicken the tail of the distribution of $G(z^{(f)})$ (without changing its mean), so that the threshold is more easily surpassed. The self-nonself distinction may, according to this model, be roughly described as follows. For a given antigen (foreign or self), finding a highly-stimulating T-cell receptor is a rare event; but if it occurs to a foreign antigen, it occurs many times simultaneously since there are numerous copies, which all contribute the same large signal, since all receptors of the T-cell involved are identical; the resulting stimulation rate is thus high. In contrast, if it is a self antigen that finds a highly-stimulating receptor, the effect is less pronounced due to the smaller copy numbers. In this sense, the toy model explains the distinction solely on the basis of copy numbers; but see the Discussion for more sophisticated effects that alleviate this requirement.

Following these intuitive arguments, we now aim at a more detailed picture of how the self background looks, and how the foreign type stands out against it. To investigate this, it is useful

rate $\setminus g_{\mathrm{act}}$	0	100	250	500	1000
variable	66.6	74.9	77.1	78.8	80.0
constitutive	22.2	59.2	277.7	590.6	1160

rate $\setminus g_{\mathrm{act}}$	0	100	250	500	1000
variable	12.7	13.9	14.5	14.9	15.1
constitutive	23.1	35.6	88.8	134.9	191.3

Table 1 Sample means (left) and sample standard deviations (right) of the histograms in Fig. 10 (left) and Fig. 11 (i.e., the self-only case).

rate $\setminus g_{\mathrm{act}}$	0	100	250	500	1000
variable	65.9	74.1	74.2	76.2	78.4
constitutive	21.8	55.9	129.5	270.4	821.1
foreign	0.9	4.0	184.8	279.6	302.2

rate $\setminus g_{\mathrm{act}}$	0	100	250	500	1000
variable	12.7	14.1	13.9	14.2	14.7
constitutive	22.4	42.0	90.4	109.1	163.7
foreign	6.7	18.5	112.2	54.5	39.2

Table 2 Sample means (left) and sample standard deviations (right) of the histograms in Fig. 10 (right) and Fig. 12 (i.e., the case with foreign antigens).

to consider the histograms of the total constitutive, variable, and foreign stimulation rates, i.e., the contributions of the constitutive sum, the variable sum, and the individual foreign term in the sum (3), either for all samples or for the subset of samples for which $G(z_f) \geq g_{\mathrm{act}}$, for various g_{act}. Since this requires a higher resolution (and thus larger sample size) than the calculation of the activation probabilities alone, such analysis would be practically impossible with simple sampling. With IS, we again generated 10000 samples per g_{act} value, from which between 30 and 70 percent turned out to reach the threshold.
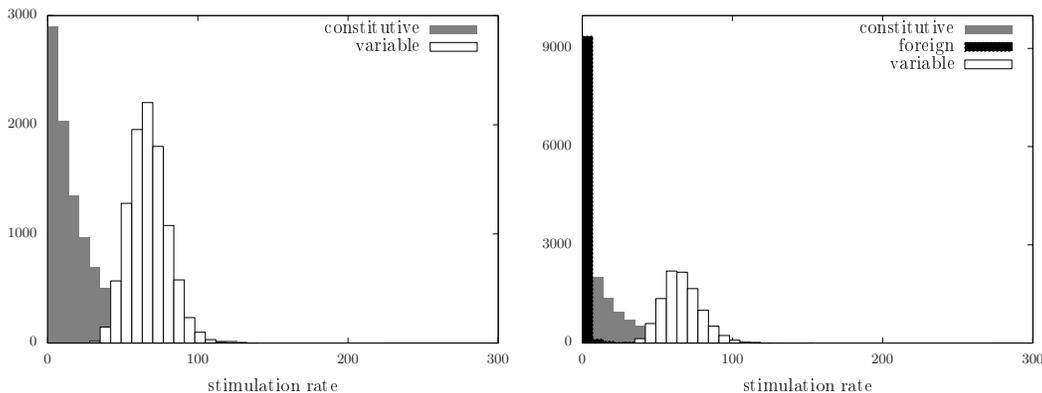

Fig. 10 Histograms of the total stimulation rates of variable, constitutive, and foreign antigens, for $z^{(f)} = 0$ (left) and $z^{(f)} = 1000$ (right), in the basic model (3), when all samples are included. Sample size is 10000, and the vertical axis holds the number of samples whose total constitutive (variable, foreign) stimulation rates fall into given intervals. Note that the scaling of the vertical axis varies across diagrams.

Figure 10 shows the resulting histograms when all samples are included, and Figs. 11 and 12 show the histograms for the subset of samples that have surpassed four representative threshold values, without and with foreign antigen. Tables 1 and 2 summarise these results in terms of means and standard deviations. Finally, Fig. 13 shows the corresponding two-dimensional statistics for all pairs of variable, constitutive, and foreign stimulation rates, again for various threshold values. (Figs. 11–13 are based on the outcome of importance sampling *without reweighting*; normalising by the number of "successful" samples would result in an estimate of the conditional distribution, because the reweighting factors cancel out.)

Let us start with the situation without foreign antigens, as displayed in Figs. 10 (left) and 11 as well as Table 1. This already illustrates the fundamental difference between variable and constitutive antigens. Judging from the large number ($m^{(v)} = 1500$) of individual terms in the sum at low copy number ($z^{(v)} = 50$), the variable stimulation rate is expected to be approximately
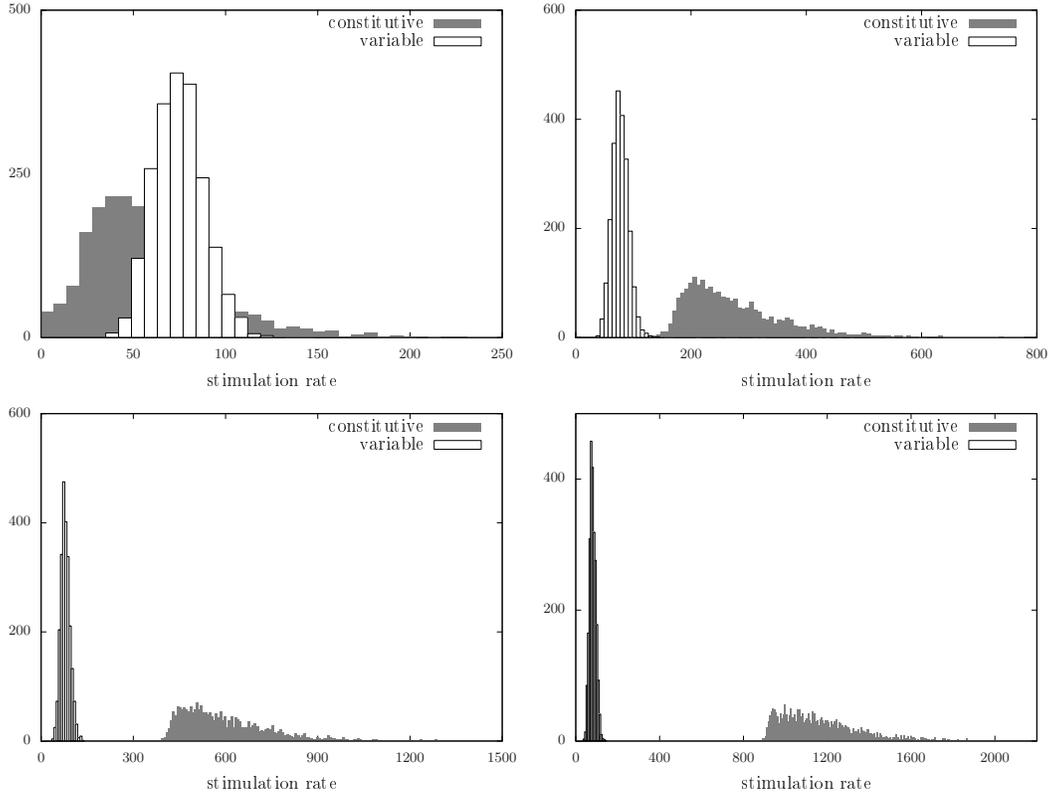
Fig. 11 Histograms of the total stimulation rates of variable and constitutive antigens, for $z^{(f)} = 0$, in the basic model (3), for samples that reach a given threshold value ($g_{\text{act}} = 100$ (upper left), $g_{\text{act}} = 250$ (upper right), $g_{\text{act}} = 500$ (lower left), $g_{\text{act}} = 1000$ (lower right)). Sample size is 10000, and the vertical axis holds the number of samples that reach g_{act} and whose total constitutive (variable, foreign) stimulation rates falls into given intervals. Note that the scaling of both axes varies across diagrams.

normally distributed and fairly closely peaked around its mean – at least as long as no restriction on $G(z^{(f)})$ is involved – and, as the Figure shows, this feature persists when $G(z^{(f)}) > g_{\text{act}}$, practically independently of the threshold involved. So, the variable antigens form a kind of background that poses no difficulty to foreign-self distinction: it is not very noisy, and it does not change with the threshold.

In contrast, the distribution of the constitutive activation rates is wider; this is due to the large copy numbers ($z^{(c)} = 500$), the effect of which is not compensated by the smaller number of terms, $m^{(c)} = 50$. Furthermore, the normal approximation is not expected to be particularly good for the constitutive antigens – given the extreme asymmetry of the W-distribution (see Fig. 3), the central limit theorem will not average out the deviations at only $m^{(c)} = 50$. In particular, the distribution remains asymmetric. With increasing threshold, this distribution moves to the right. The reason for this is that, in order to reach an increasing g_{act}, the tail events of the constitutive or the variable sum or both must be used, but it is "easier" (that is, more probable) to use the constitutive one because it contains more atypical events. In the language of large deviation theory, this is an example of the general principle that "large deviations are always done in the the least unlikely of all the unlikely ways" [8, Ch. I]. In the language of biology, the constitutive antigens are the problem of foreign-self distinction: due to their high copy numbers and incomplete averaging, fluctuations persist that occasionally induce an immune response even in the absence of foreign antigens. This occurs if a T-cell receptor happens to fit particularly well to one, or a number of, constitutive antigen types on an APC; due to their large copy numbers,
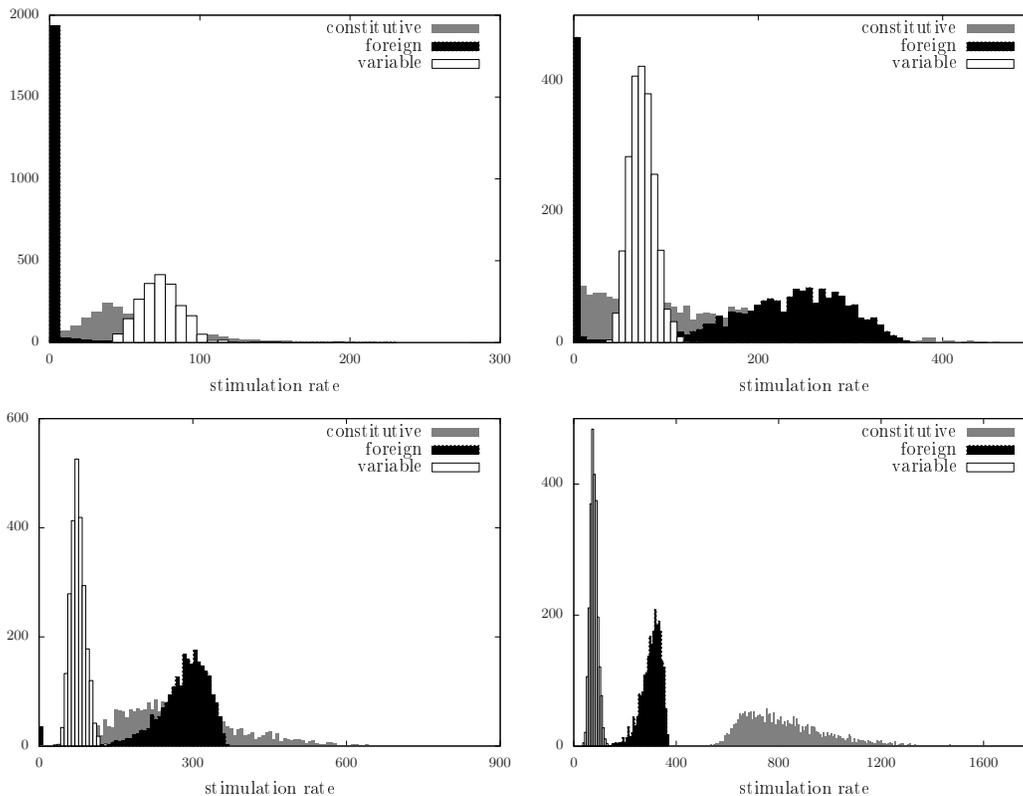
Fig. 12 Histograms of the total constitutive, variable and foreign stimulation rates for $z^{(f)} = 1000$ in the basic model (3). Sample size is 10000, and the vertical axis holds the number of samples that reach the threshold g_{act} and whose total constitutive (variable, foreign) stimulation rate falls into a given interval, for $g_{\text{act}} = 100$ (upper left), $g_{\text{act}} = 250$ (upper right), $g_{\text{act}} = 500$ (lower left), $g_{\text{act}} = 1000$ (lower right). The maximal stimulation rate for the foreign antigens is $z^{(f)} w(1) = 367.9$. Note that the scaling of both axes varies across diagrams.

these few highly-stimulating types are then sufficient to surpass the threshold (in contrast, several highly-stimulating types would be required for the variable antigens to elicit a reaction, which is too improbable).

Let us now turn to the picture with foreign antigen present (Figs. 10 (right), 12, 13, and Table 2). One salient feature here is that the variable stimulation rate behaves exactly as in the self-only case: closely peaked around a small mean, unchanged when $\{G(z^{(f)}) > g_{\text{act}}\}$ is imposed. The picture is thus dominated by the interplay of constitutive and foreign types. In line with Fig. 5, the situation is similar in the case without restriction on $G(z^{(f)})$ (Fig. 10, right) and the case when $G(z^{(f)}) \geq 100$ (Fig. 12, upper left). In particular, the foreign stimulation rate is closely peaked at 0; only the constitutive background has moved slightly to the right, exactly as in the self-only case. For $g_{\text{act}} = 250$ (Fig. 12, upper right), where, according to Fig. 5, foreign-self distinction sets in, the foreign stimulation rate becomes prominent: the right branch of the W-distribution now becomes populated, and the associated stimulation rates are large due to the large copy numbers $z^{(f)}$ involved.

Nevertheless, for $g_{\text{act}} = 250$, the foreign stimulation rate is close to 0 in a sizable fraction of the cases in which an immune reaction occurs – here, the reaction is brought about by the constitutive background, which moves to the right just as in the self-only case (but less pronounced). Fig. 13 shows that the constitutive and foreign stimulation rates are, indeed, negatively correlated: as is to be expected, low foreign rates are compensated by high constitutive rates and vice versa

(in contrast, the variable background hardly correlates with either the constitutive or the foreign stimulation rate). As in the self-only case, therefore, the level of unwanted activation ("self-only" or "mainly self, without appreciable foreign activation") is set by the tail behaviour of the constitutive background. However, if g_{act} is increased further (Fig. 12, lower left), every T cell beyond the threshold displays high stimuli for the foreign antigen, their distribution shifting even further to the right and concentrating near the maximal stimulation rate given by the maximum of the function w of Eq. (1), more precisely, by $z^{(f)}w(1)$. This maximum can, of course, not change by imposing restrictions on $G(z^{(f)})$; thus, any further increase of g_{act} (Fig. 12, lower right) must then be matched by the by now familiar shift of the constitutive background. (This last panel is, however, less biologically realistic since the probabilities involved are too small to be relevant – after all, with about 10^7 different T-cell types, threshold values that yield activation probabilities far below 10^{-7} even in the presence of foreign antigens offer no immune protection.)

A further illustration of the onset of self-nonself distinction is presented in Fig. 14. Here we consider

$$\mathbb{P}\big(G(z^{(f)}) - z^{(f)}W_{n^{(c)}+n^{(v)}+1} > g_{\text{act}} \mid G(z^{(f)}) > g_{\text{act}}\big) = \frac{\mathbb{P}\big(G(z^{(f)}) - z^{(f)}W_{n^{(c)}+n^{(v)}+1} > g_{\text{act}}\big)}{\mathbb{P}\big(G(z^{(f)}) > g_{\text{act}}\big)},$$

$$(39)$$

i.e., the probability that, in a T-cell that is activated in the presence of foreign antigen, the self component alone would have been sufficient for the activation. From $z^{(f)} = 1000$ onwards, this probability decreases to 0 quickly with increasing g_{act}. Put differently, in large parameter regions, the foreign antigens do indeed make the difference, which is the decisive feature of self-nonself distinction.

6 Conclusion and outlook

We have established here a method of LD sampling that allows the convenient simulation of the rare events relevant to statistical recognition in the immune system. Thus a more thorough investigation of these events could be carried out.

But this is only a first step, and the goal for future work is to use this or related methods to investigate biologically realistic models. Indeed, the toy model considered here, which relies solely on distinction by copy numbers, does serve the aim to illustrate that distinction against a noisy background is, at all, possible, even without an intrinsic difference between self and nonself, and how this is related to the rare events in the tail of the background distribution. However, biologically realistic models have to take into account tolerisation mechanisms that make the T-cells less responsive to self antigens. One important such mechanism is so-called *negative selection*. Negative selection occurs during the maturation phase of young T-cells in the thymus, before they are released into the body. In a process similar to the one described by the toy model, they are confronted with APCs that present mixtures of various self antigens, and those T-cells whose activation rate surpasses a thymic activation threshold $g_{\text{thy}} < g_{\text{act}}$ are eliminated. When they are later, after leaving the thymus, confronted with mixtures of self and foreign antigens, the stimulation rates emerging from self and foreign are no longer i.i.d. (the self ones are biased towards smaller values and possibly negatively correlated). In fact, a simple model for negative selection was already described in BRB [33], and shown to drastically reduce the self background, so that foreign antigens do no longer require elevated copy numbers to be detected. More sophisticated models of negative selection have been formulated e.g. in [32]. However, their simulation still awaits the development of adequate methods. This is the purpose of ongoing work.
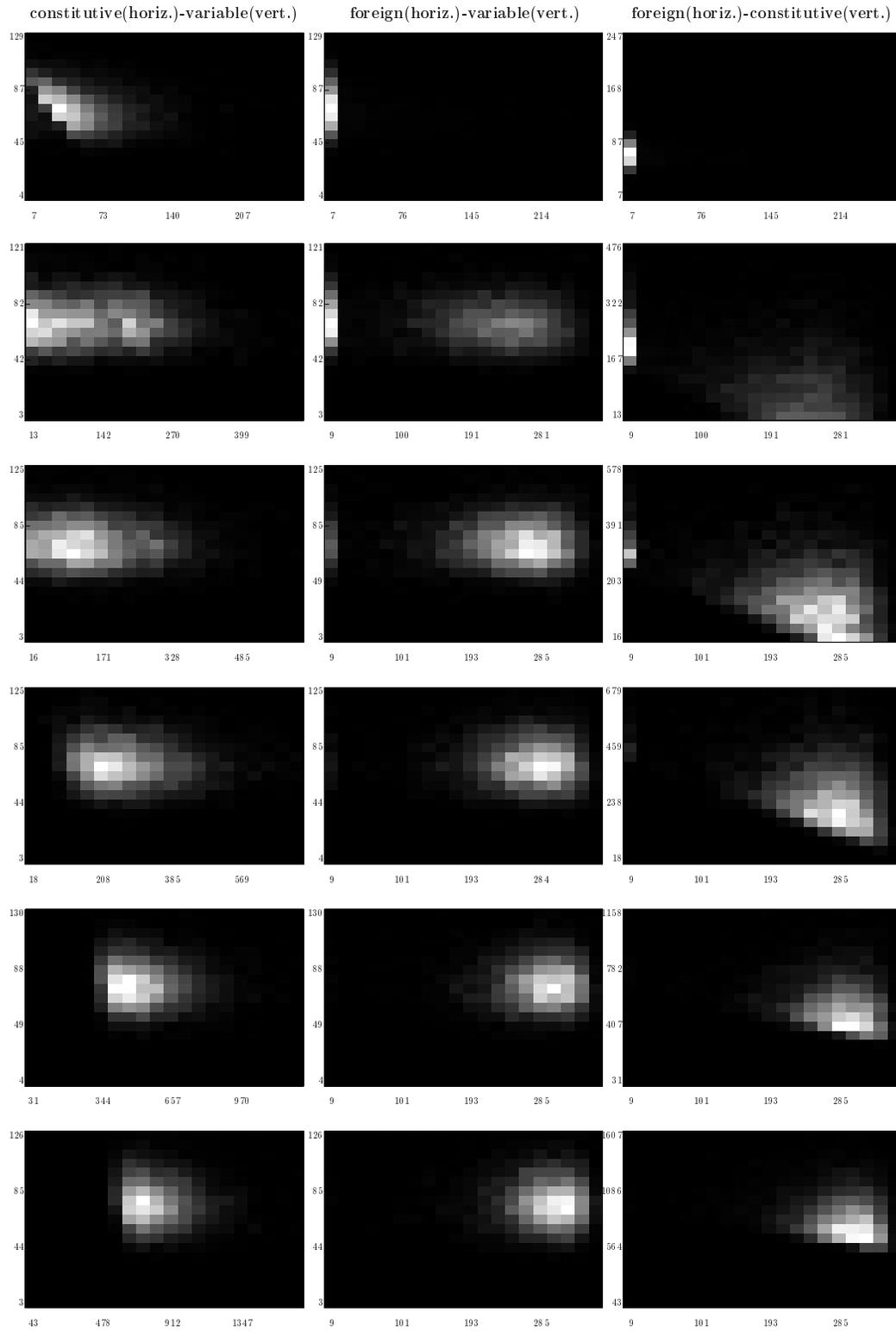
7 Acknowledgements

Fig. 13 Pairwise joint frequencies of the total constitutive, variable, and foreign stimulation rates, for those samples with $G(z^{(f)}) > g_{\mathrm{act}}$ in the basic model (3) (with $z^{(f)} = 1000$). Greyscales correspond to number of samples falling into 2D-intervals defined by total stimulation rates of pairs of antigen types. Rows (from top to bottom): $g_{\mathrm{act}} = 100, 250, 350, 500, 750, 1000$; columns (from left to right): constitutive (horizontal) – variable (vertical); foreign (horizontal) – variable (vertical); foreign (horizontal) – constitutive (vertical). Lighter shading corresponds to higher frequencies.
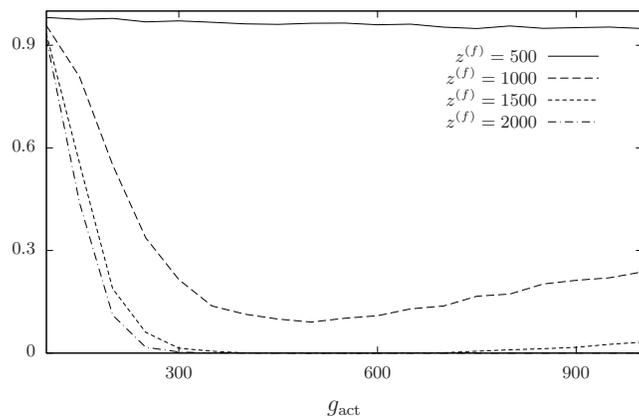
Fig. 14 Fraction of samples whose self-component alone is above threshold, among those that reach the threshold in the presence of $z^{(f)}$ foreign molecules, for various $z^{(f)}$ (i.e., IS simulation of the probability in Eq. (39)). Sample size is 10000 for each g_{act} value considered.

References

1. Arstila, T., Casrouge, A., Baron, V., Even, J., Kannelopoulos, J., Kourilsky, P.: A direct estimate of the human $\alpha\beta$ T cell receptor diversity. Science **286**, 958–961 (1999).
2. Asmussen, S.: Applied Probability and Queues. 2nd ed., Springer, New York (2003).
3. Billingsley, P.: Probability and Measure. 3rd ed., Wiley, New York (1995).
4. Borovsky, Z., Mishan-Eisenberg, G., Yaniv, E., Rachmilewitz, J.: Serial triggering of T cell receptors results in incremental accumulation of signaling intermediates. J. Biol. Chem. **277**, 21529–21536 (2002).
5. Bucklew, J.A.: Introduction to Rare Event Simulation. Springer, New York (2004).
6. Davis, S.J., Ikemizu, S., Evans, E.J., Fugger, L., Bakker, T.R., van der Merwe, P.A.: The nature of molecular recognition by T cells. Nat. Immunol. **4**, 217–224 (2003).
7. Dembo, A., Zeitouni, O.: Large Deviations Techniques and Applications. Springer, New York (1998).
8. den Hollander, F.: Large Deviations. AMS, Providence, RI (2000).
9. Dieker, A., Mandjes, M.: On asymptotically efficient simulation of large deviation probabilities. Adv. Appl. Prob. **37**, 539–552 (2005).
10. Dushek, O., Coombs, D.: Analysis of serial engagement and peptide-MHC transport in T cell receptor microclusters. Biophys. J. **94**, 3447–3460 (2008).
11. Georgii, H.O.: Stochastics. de Gruyter, Berlin (2008).
12. Gonzalez, P.A., Carreno, L.J., Coombs, D., Mora, J.E., Palmieri, E., Goldstein, B., Nathenson, S.G., Kalergis, A.M.: T-cell receptor binding kinetics required for T cell activation depend on the density of cognate ligand on the antigen-presenting cell. Proc. Natl. Acad. Sci. U.S.A **102**, 4824–4829 (2005).
13. Hlavacek, W.S., Redondo, A., Wofsy, C., Goldstein, B.: Kinetic proofreading in receptor-mediated transduction of cellular signals: receptor aggregation, partially activated receptors, and cytosolic messengers. Bull. Math. Biol. **64**, 887–911 (2002).
14. Hunt, D. F., Henderson, R.A., Shabanowitz, J., Sakaguchi, K., Michel, H., Sevilir, N., Cox, A.L., Appella, E., Engelhard, V.H.: Characterization of peptides bound to the class I MHC molecule HLA-A2.1 by mass spectrometry. Science **255** (1992), 1261–1263.
15. Kalergis, A.M., Boucheron, N., Doucey, M.A., Palmieri, E., Goyarts, E.C., Vegh, Z., Luescher, I.F., Nathenson, S.G.: Efficient T cell activation requires an optimal dwell-time of interaction between the TCR and the pMHC complex. Nat. Immunol. **2**, 229–234 (2001).
16. Kronmal, R.A., Peterson, A.J.: On the alias method for generating random variables from a discrete distribution. Amer. Stat. **33**, 214–218 (1979).
17. Lancet, D., Sadovsky, E., Seidelmann, E.: Probability model for molecular recognition in biological receptor repertoires: Significance to the olfactory system. Proc. Natl. Acad. Sci. U.S.A. **90**, 3715–3719 (1993).
18. Lord, G.M., Lechler, R.I., George, A.J.: A kinetic differentiation model for the action of altered TCR ligands. Immunol. Today **20**, 33–39 (1999).
19. Madras, N.: Lectures on Monte-Carlo Methods. AMS, Providence, RI (2002).
20. Mason, D.: A very high level of crossreactivity is an essential feature of the T-cell receptor. Immunol. Today **19**, 395–404 (1998).
21. McKeithan, T.W.: Kinetic proofreading in T-cell receptor signal transduction. Proc. Natl. Acad. Sci. U.S.A. **92**, 5042–5046 (1995).
22. Rabinowitz, J.D., Beeson, C., Wulfing, C., Tate, K., Allen, P.M., Davis, M.M., McConnell, H.M.: Altered T-cell receptor ligands trigger a subset of early T cell signals. Immunity **5**, 125–135 (1996).
23. Rosenwald, S., Kafri, R., Lancet, D.: Test of a statistical model for molecular recognition in biological repertoires. J. Theor. Biol. **216**, 327–336 (2002).
24. Ross, S.M.: Simulation. Academic Press (2002).
25. Rothenberg, E.V.: How T-cells count. Science **273**, 78–80 (1996).
26. Sadowsky, J.S., Bucklew, J.A.: On large deviations theory and asymptotically efficient Monte Carlo estimation. IEEE TIT **36**, 579–588 (1990).
27. Sousa, J., Carneiro, J.: A mathematical analysis of TCR serial triggering and down-regulation. Eur. J. Immunol. **30**, 3219–3227 (2000).
28. Stevanovíc, S., Schild, H.: Quantitative aspects of T cell activation – peptide generation and editing by MHC class I molecule. Seminars Immunol. **11** (1999), 375–384.
29. Utzny, C., Coombs, D., Muller, S., Valitutti, S.: Analysis of peptide/MHC-induced TCR downregulation: deciphering the triggering kinetics. Cell Biochem. Biophys. **46**, 101–111 (2006).
30. Valitutti, S., Lanzavecchia, A.: Serial triggering of TCRs: a basis for the sensitivity and specificity of antigen recognition. Immunol. Today **18**, 299–304 (1997).
31. Valitutti, S., Muller, S., Cella, M., Padovan, E., Lanzavecchia, A.: Serial triggering of many T-cell receptors by a few peptide-MHC complexes. Nature **375**, 148–151 (1995).
32. van den Berg, H.A., Molina-París, C.: Thymic presentation of autoantigens and the efficiency of negative selection. J. Theor. Med. **5**, 1–22 (2003).
33. van den Berg, H.A., Rand, D.A., Burroughs, N.J.: A reliable and safe T-cell repertoire based on low-affinity T-cell receptors. J. Theor. Biol. **209**, 465–486 (2001).
34. van den Berg, H.A., Rand, D.A.: Antigen presentation on MHC molecules as a diversity filter that enhances immune efficacy. J. Theor. Biol. **224**, 249–267 (2003).

35. van den Berg, H.A., Rand, D.A.: Quantitative theory of T-cell responsiveness. Immunol. Rev. **216**, 81–92 (2007).
36. Viola, A., Lanzavecchia, A.: T-cell activation determined by T-cell receptor number and tunable thresholds. Science **273**, 104–106 (1996).
37. Zint, N., Baake, E., den Hollander, F.: How T-cells use large deviations to recognize foreign antigens. J. Math. Biol. **57**, 841–861 (2008).